A fast upper envelope scan method for discrete-continuous dynamic programming*

Loretti I. Dobrescu† and Akshay Shanker ‡

First draft: August 4, 2022

Current draft: October 21, 2024

Abstract

We develop a general fast upper envelope scan method to solve any stochastic dynamic models with discrete-continuous choices where the optimization problem has a one-dimensional representation. For this vast class of models, FUES enables the endogenous grid method by efficiently selecting the optimal solution using a targeted secant scan. Importantly, it does so without requiring either monotonicity of the policy function or analytical information on the value function gradient. We demonstrate our method using several workhorse applications in the literature, and show the massive computational speed and accuracy gains generated across the board, even when uncertainty may lead to highly complex endogenous grids of potential solution points.

Key Words: discrete-continuous choices, non-convex optimization, Euler equation, stochastic dynamic programming

JEL Classification: C13, C63, D91

* We thank Hazel Bateman, Chris Carroll, Mike Keane, Ben Newell, Ben Moll, John Rust, Fedor Ishkakov, Greg Kaplan, Bertel Schjerning, Susan Thorp, Anant Mathur, Mateo Velasquez-Giraldo, and conference and seminar participants at several institutions for valuable feedback, discussions and comments. Research support from the Australian Research Council (ARC LP150100608) and ARC Centre of Excellence in Population Ageing Research (CE17010005) is gratefully acknowledged. This research was undertaken with the assistance of resources and services from the National Computational Infrastructure (NCI), which is supported by the Australian Government. The software implementing FUES in our applications, as well as the one providing the function that implements FUES in its general form can be found at here.

†Corresponding author. School of Economics, University of New South Wales, Australia. Email: dobrescu@unsw.edu.au.

‡School of Economics, University of New South Wales, Australia. Email: a.shanker@unsw.edu.au.

1 Introduction

Stochastic dynamic decision-making applications have increasingly been incorporating discrete-continuous choices. Such choices are central to understanding the dynamics of investment frictions (Skiba, 1978; Khan and Thomas, 2008), housing adjustments (Yogo, 2016; Kaplan et al., 2020), the implications of durable goods consumption for macroeconomic dynamics (Kaplan and Violante, 2014; Berger and Vavra, 2015), life-cycle asset allocation (Fagereng et al., 2019; Laibson et al., 2021), labour supply (Attanasio et al., 2018; Iskhakov and Keane, 2021) or default risk (Arellano, 2008; Arellano et al., 2016; Jang and Lee, 2023), to name just a few areas of active research.

Currently, the standard approach to solve stochastic dynamic problems is the endogenous grid method (EGM). Unlike value function iteration (VFI), EGM relies on analytically inverting the Euler equation (Carroll, 2006) and may completely remove costly numerical root-finding or optimization steps (Iskhakov, 2015). The drawback however is that, similar to other Euler equation methods (Coleman, 1990; Li and Stachurski, 2014), EGM relies on the value function concavity to ensure Euler equation solutions are globally optimal. This concavity breaks down in models involving both continuous and discrete choices, leading to sub-optimal Euler equation solutions due to discontinuous policy functions (Fella, 2014; Iskhakov et al., 2017). Several one-dimensional methods have been suggested so far to calculate the upper envelope of the solutions generated by EGM (Fella, 2014; Iskhakov et al., 2017; Druedahl and Jørgensen, 2017; Druedahl, 2021). All these methods, however, either depend on monotonicity of the policy function (Iskhakov et al., 2017; Fella, 2014), or rely on combining numerical optimization with Euler equation methods (Druedahl, 2021) that can lead to loss of computational accuracy and efficiency.

We address these challenges by developing a general and efficient method to compute the upper envelope of the value correspondence generated by EGM for problems where current period states can be collapsed to one-dimensional ones. Our fast upper envelope scan (FUES) method works by noting that the upper envelope of the value correspondence is the supremum of choice-specific concave value functions, with each value function corresponding to a history-dependent future sequence of discrete choices. The convex regions of the upper envelope occur where different choice-specific value functions cross, with the optimal policy function experiencing discontinuous jumps only in these regions. As a result, FUES performs a secant scan to determine whether including a potential optimal point forms a concave or convex region of the upper envelope. If it forms a concave region, the point is eliminated as sub-optimal if it induces a jump in the policy function. If,

however, it forms a convex region of the upper envelope, the candidate point is considered optimal and retained.

We illustrate the wide applicability of our method via three applications. First, we implement FUES in a classic discrete-continuous dynamic model - i.e., a life-cycle model with discrete retirement and continuous consumption decisions à la Iskhakov et al. (2017). Second, we apply FUES to a problem of continuous housing investment with adjustment frictions where previous methods fail due to the non-monotonicity of the policy function. Featuring both liquid and illiquid assets, this example also shows how our method can be applied to multidimensional problems that do not satisfy the conditions for 'pure EGM' (Iskhakov, 2015), by breaking up such problems into a one-dimensional EGM step and a root-finding step. Finally, the third application uses FUES in an infinite horizon model with discrete housing and continuous liquid assets (Fella, 2014).

For each application, we compare the performance of FUES against widely-used one-dimensional methods such as DC-EGM (Iskhakov et al., 2017) and nested-EGM (NEGM, Druedahl (2021)), as well as against the multidimensional rooftop-cut method (RFC, Dobrescu and Shanker (2024)). In all cases, FUES demonstrates a considerable computational speed advantage. For instance, when computing the upper envelope, FUES is up to an order of magnitude faster compared to both DC-EGM and RFC. For NEGM, since it is not an upper envelope method, we compare directly the overall solution times to find FUES delivering average speed gains of about 50%. Finally, FUES's speed advantage is particularly notable in less stylized optimization problems, where the endogenous grid of potential solutions may be non-monotone *even if the optimal policy function is monotone* - e.g., in models with uncertainty that 'smooth' (potentially multiple) discrete choices and likely introduce infinite Euler equation roots in non-concave regions of the value function. Specifically, we find the added complexity of the 'logit smoothing' previously employed in our first application to significantly hamper DC-EGM, giving FUES a 10x speed advantage that remains stable across model parametrizations. As for accuracy, FUES performs on average better than both DC-EGM and NEGM in terms of Euler equation error. When DC-EGM can be applied, the accuracy gains of FUES over DC-EGM are more modest because both methods calculate the upper envelope using the analytical inverse of the Euler equation. In contrast, FUES achieves up to an order of magnitude improvement in Euler error over NEGM as it eliminates the need for numerical optimization.

Next, we provide a theoretical foundation for FUES in its general form, showing how it can recover the optimal value function without error when (i) the jumps between policy functions are bounded below (as is the case when there are finitely many jumps in the

policy functions), (ii) the grid size is sufficiently large relative to the size of the policy function jumps, and (iii) the endogenous grid behaves well around the crossing points between choice-specific value functions. The first two conditions are straightforward to verify in practice, and ensure FUES can differentiate between jumps in the policy function that reflect shifts in future discrete choices and smooth changes in policy along a given choice sequence. The third condition ensures that the intersection points of the value functions are correctly identified as optimal or sub-optimal and may be harder to verify. To address potential violations of this assumption, we incorporate in the FUES algorithm both 'forward' and 'backward' scans, which help ensure its robust performance even when all the underlying assumptions are not fully satisfied.

FUES advances considerably the latest methods to solve discrete-continuous dynamic models (Fella, 2014; Iskhakov et al., 2017; Druedahl, 2021; Dobrescu and Shanker, 2024). Both Fella (2014) and Iskhakov et al. (2017) rely on the monotonicity of the optimal policy functions, while Druedahl (2021) requires a nested numerical optimization step or is tied to a particular interpolation method. In contrast, the RFC implemented in Dobrescu and Shanker (2024) requires analytical information on the gradient of the policy function and also performs a potentially complex nearest neighbour search at each grid point. In this respect, our method advances the literature in several ways. First, FUES does not require the monotonicity of any of the policy functions. Second, since FUES operates on (and returns) a single dimensional array regardless of model complexity, it is highly compatible with cutting-edge massively parallel and efficiently vectorized computing using languages such as `Google JAX`, `Numba` and `NumPy`. Finally, FUES is considerably easier to implement, and does not require knowing the shape of the policy functions or the gradient of the value function. Our numerical results suggest FUES is well-suited to compute the upper envelope in discrete-continuous problems featuring uncertainty, which covers a broad set problems found in recent literature, including those studying fiscal policy transmission (Brumm et al., 2024), the effect of durable goods on the marginal propensity to spend (Kovacs et al., 2021; Beraja and Zorzi, 2024), the distribution of homeownership (Le Blanc et al., 2023) and labour market choices (Cruces, 2024; Bacher et al., 2024).

The paper proceeds as follows. In Section 2, we start by solving and discussing our main results in the context of three well-known applications. Section 2.1 introduces FUES informally using the simple retirement choice model in Iskhakov et al. (2017) where agents choose their savings and labor force participation; here we also compare the performance of FUES to that of the DC-EGM method proposed by Iskhakov et al. (2017). Section 2.2 further demonstrates FUES in an application where DC-EGM fails, using a model in which

agents choose whether or not to adjust their illiquid housing assets. Finally, Section 2.3 showcases FUES in the discrete choice model proposed by Fella (2014) where agents decide to hold liquid and illiquid assets via discrete choices. In Section 3, we follow our study of these applications by formally stating FUES in its general form and providing the proofs on how FUES obtains the upper envelope. Section 4 concludes.

2 Illustrative applications

We start by introducing FUES in the context of three well-known dynamic optimization applications. After briefly introducing each problem, we discuss how their discrete choices result in non-convexity, and show how FUES can retrieve the optimal solution.

2.1 Application 1: Retirement choice

2.1.1 Model environment

Consider the finite horizon retirement and savings choice model in Iskhakov et al. (2017) where an agent consumes, works (if they so choose), and saves from time $t = 0$ until time $t = T$. At the beginning of each period, the agent starts as a worker or retiree, with the state variable denoting their beginning-of-period work status given by the discrete variable d_t. If the agent works, they earn a per-period wage y. Every period, the agent can choose to continue working during the next period by setting $d_{t+1} = 1$, or to permanently exit the workforce by setting $d_{t+1} = 0$. If the agent chooses to work the next period, they will incur a utility cost δ at time t. We assume all agents start as workers so $d_0 = 1$. Agents can also consume c_t and save in liquid (financial) assets a_t, with $a_t \in S$ and $S := [0, \bar{a}] \subset \mathbb{R}_+$. Thus, the intertemporal budget constraint is

$$a_{t+1} = (1 + r)a_t + d_t y - c_t. \tag{1}$$

Per-period utility is given by $\log(c_t) - \delta d_t$. Letting the function u be defined by $u(c) = \log(c)$, the agent's maximization problem becomes

$$V_0^{d_0}(a_0) = \max_{(c_t, d_{t+1})_{t=0}^T} \left\{ \sum_{t=0}^{T} \beta^t u(c_t) - \delta d_{t+1} \right\}, \tag{2}$$

subject to Equation (1), $a_t \in S$ for each t, and the fact that the agent cannot return to work after retiring (i.e., $d_{t+1} = 0$ if $d_t = 0$). Let $V_t^{d_t}$ denote the beginning-of-period value

function. If the agent enters the period as a worker, the agent's time t value function will be characterised by the Bellman equation

$$V_t^1(a) = \max_{c, d_{t+1} \in \{0,1\}} \left\{ u(c) - d_{t+1}\delta + \beta V_{t+1}^{d_{t+1}}(a') \right\}, \tag{3}$$

where $a' = (1+r)a + y - c$ and $a' \in S$. If the agent enters the period as a retiree, the value function becomes

$$V_t^0(a) = \max_{c} \left\{ u(c) + \beta V_{t+1}^0(a') \right\}, \tag{4}$$

with $a' = (1+r)a - c$. The optimization problem for the retiree is a standard concave problem. For the worker, however, the optimization problem is not concave since she optimizes jointly a discrete choice and a continuous choice. Moreover, even conditional on $d_{t+1} = 1$, next period value function V_{t+1}^1 will not be concave since the value function represents the supremum over *all future feasible combinations of discrete choices*. The non-concavity of V_{t+1}^1 produces the 'secondary kinks' described by Iskhakov et al. (2017).

To see how the choice at time t implicitly controls the future sequence of discrete choices and produces the secondary kinks, write the time t worker's value function as

$$V_t^1(a) = \max_{c} \max_{\mathbf{d} \in \mathbb{D}} \left\{ u(c) + \beta Q_{t+1}^{\mathbf{d}}(a') \right\}, \tag{5}$$

where $Q_{t+1}^{\mathbf{d}}$ is the $t+1$ value function conditional on a given sequence of future discrete choices $\mathbf{d}$, with $\mathbf{d} = \{d_{t+1}, d_{t+2}, \ldots, d_T\}$. In particular, letting $\bar{\delta} = \{\delta, \beta\delta, \beta^2\delta, \ldots, \beta^{T-1}\delta\}$, we have

$$Q_{t+1}^{\mathbf{d}}(a) = \max_{(c_k)_{k=t+1}^T} \left\{ \sum_{k=t+1}^{T} \beta^t u(c_k) \right\} - \bar{\delta}^T \mathbf{d}. \tag{6}$$

To sum up, the value function non-concavity, even holding the choice d_{t+1} fixed, is brought on by the implicit changes in the entire future sequence of discrete choices as one controls the choice variable c in (5). In this case, the Bellman equation (3) still holds, and one can numerically implement VFI to compute a solution. The challenge arises when solving the Bellman equation using numerical methods becomes burdensome computationally. A more computationally efficient strategy involves recovering the policy function by solving for points that satisfy the first order conditions (FOCs - i.e., the Euler equations) of the Bellman equation. However, since the upper envelope is not concave, the points satisfying the FOCs could be associated with any future sequence of discrete choice in Figure 1, and may not be on the upper envelope.

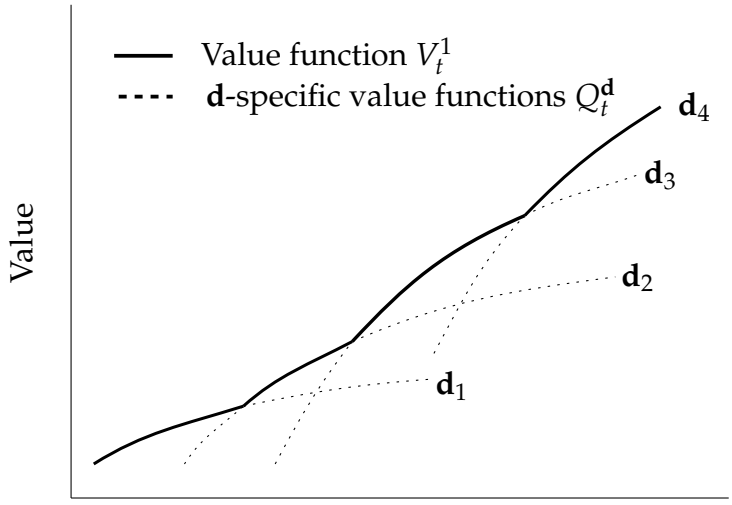

Figure 1: The time t worker value function V_t^1 is the upper envelope of concave functions, where each concave function is a value function conditional on a *sequence* of future discrete choices. The subscript 'i' on $\mathbf{d}_i$ indicate distinct sequences of future discrete choices.

2.1.2 The Euler equations

We now discuss the FOCs and then proceed to our contribution (i.e., the FUES method) as a way to use necessary first order information to efficiently compute V_t. If the agent chooses $d_{t+1} = 1$ (i.e., they continue as a worker in $t+1$), we can write the time t worker Euler equation as

$$u'(c_t^1) \geq \beta(1+r)u'(c_{t+1}),$$

where c_t^1 is the time t consumption policy conditional on $d_{t+1} = 1$, while c_{t+1} is the unconditional time $t+1$ consumption policy. On the other hand, if the agent chooses $d_{t+1} = 0$ (i.e., they retire), then the Euler equation is

$$u'(c_t^0) \geq \beta(1+r)u'(c_{t+1}^0).$$

Functional Euler equations. It will now be helpful to write the Euler equation in its functional form. Let $\sigma_t^d : S \times \{0,1\} \to \mathbb{R}_+$ be the conditional asset policy function for the worker at time t if $d = 1$, and for the retiree if $d = 0$. We call σ_t^d the conditional policy because it will depend, through its second argument, on the discrete choice (to work or not to work in $t+1$) made by the worker at time t. The time t and time $t+1$ policy

functions will satisfy the following functional Euler equation:

$$u'((1+r)a + dy - \sigma_t^d(a, d_{t+1})) \\ \geq \beta(1+r)u'((1+r)\sigma_t^d(a, d_{t+1}) + d_{t+1}y - \sigma_{t+1}^{d_{t+1}}(a', d_{t+2})), \quad (7)$$

where $a' = \sigma_t^d(a, d_{t+1})$. On the choice of whether to work or not, the time t worker will chose $d_{t+1} = 1$ if and only if

$$u((1+r)a + y - \sigma_t^1(a,1)) - \delta + \beta V_{t+1}^1(\sigma_t^1(a,1)) \\ > u((1+r)a + y - \sigma_t^1(a,0)) + \beta V_{t+1}^0(\sigma_t^1(a,0)). \quad (8)$$

Since the discrete choice is itself a function of the state, we can also define a discrete choice policy function $\mathcal{I}_t \colon S \times \{0,1\} \to \{0,1\}$. As such, we will have $d_{t+1} = \mathcal{I}_t(a,d)$ and $d_{t+2} = \mathcal{I}_{t+1}(a', d_{t+1})$, where $\mathcal{I}_t$ is evaluated to satisfy (8) each period conditional on the $t+1$ value function.

2.1.3 Computation using EGM and FUES

We now turn to how FUES can identify the upper envelope from a set of points that satisfy the Euler equations. Fix a time t and suppose the value function V_{t+1}^d, the discrete choice function $\mathcal{I}_{t+1}$, and the optimal policy function σ_{t+1}^d for $d = 0$ and $d = 1$ are known. Let $\hat{\mathbb{X}}_t$, $\hat{\mathbb{V}}_t$ and $\hat{\mathbb{X}}_t'$ be sequences of points satisfying the following Euler equation for workers:

$$u'((1+r)\hat{x}_i + dy - \hat{x}_i') = \beta(1+r)u'((1+r)\hat{x}_i' + yd_{t+1} - \sigma_{t+1}^{d_{t+1}}(\hat{x}_i', d_{t+2})), \quad (9)$$

$$\hat{v}_i = u((1+r)\hat{x}_i + dy - \hat{x}_i') - d\delta + V_{t+1}^d(\hat{x}_i), \quad (10)$$

where $d_{t+2} = \mathcal{I}_{t+1}(\hat{x}_i', d_{t+1})$, $\hat{x}_i \in \hat{\mathbb{X}}_t$, $\hat{v}_i \in \hat{\mathbb{V}}_t$ and $\hat{x}_i' \in \hat{\mathbb{X}}_t$. Such a sequence of points can be generated analytically using EGM. In particular, we have

$$(1+r)\hat{x}_i + dy - \hat{x}_i' = u'^{,-1}\left[\beta(1+r)u'((1+r)\hat{x}_i' + yd_{t+1} - \sigma_{t+1}^{d_{t+1}}(\hat{x}_i', d_{t+2}))\right]. \quad (11)$$

In the case of the EGM, $\hat{\mathbb{X}}_t$ is the endogenous grid of points, $\hat{\mathbb{X}}_t'$ is the exogenous one, and $\hat{\mathbb{V}}_t$ is the value correspondence.

Next, order the points in $\hat{\mathbb{X}}_t$, $\hat{\mathbb{V}}_t$ and $\hat{\mathbb{X}}_t'$ in ascending order of the *endogenous grid points* $\hat{\mathbb{X}}_t$. Consider the left panel of Figure 2 as a stylised plot of the endogenous grid points $\hat{\mathbb{X}}_t$ and associated continuation payoffs $\hat{\mathbb{V}}_t$ generated by EGM. Assume for the purpose

of illustration that the EGM points are associated with two overlapping future choice-specific value functions. The right panel of Figure 2 displays the policy functions (i.e., next period assets) associated with each future choice-specific value function. Pick a point $\hat{x}_i$, with $\hat{x}_i \in \hat{\mathbb{X}}_t$ such that $\hat{x}'_i$ is optimal given $\hat{x}_i$ and it lies on the upper envelope. Note if the points $\hat{x}_{i+1}$ and $\hat{x}'_{i+1}$ imply a different future sequence of discrete choices to $\hat{x}_i$ and $\hat{x}'_i$, then $\hat{x}'_{i+1}$ will experience a 'discontinuous jump' from $\hat{x}'_i$. However, for $\hat{x}'_{i+1}$ to be on the upper envelope, it must be that $\hat{x}'_{i+1}$ can only jump if it occurs after the crossing point between two value functions (for instance, the point $\hat{x}_6$). That is, $(\hat{x}'_{i+1}, \hat{v}_{i+1})$ can only jump if it makes a *convex* 'left turn' from the line joining $(\hat{x}'_{i-1}, \hat{v}_{i-1})$ and $(\hat{x}'_i, \hat{v}_i)$. On the other hand, if $(\hat{x}'_{i+1}, \hat{v}_{i+1})$ makes a *concave* 'right turn', it cannot jump for it to be on the upper envelope. The reason is that if $(\hat{x}'_{i+1}, \hat{v}_{i+1})$ has made a right turn, for $(\hat{x}'_{i+1}, \hat{v}_{i+1})$ to be on the upper envelope, it must be on the *concave value function* yielding the same future sequence of discrete choices $\mathbf{d}$ as implied by $(\hat{x}'_i, \hat{v}_i)$. If a right turn is associated with a jump (e.g., point $\hat{x}_7$), then it must be on a value function associated with a sub-optimal set of future discrete choices. Section 3 formally proves this argument (and provide the pseudo-code), while informally we use the intuition from Figure 2 to implement FUES as:

Box 1: FUES method

1. Compute $\hat{\mathbb{X}}_t$, $\hat{\mathbb{V}}_t$ and $\hat{\mathbb{X}}'_t$ using standard EGM.
2. Set a pre-determined 'jump detection' threshold $\bar{M}$.
3. Sort all sequences in order of the *endogenous* grid $\hat{\mathbb{X}}_t$.
4. Start from point $i = 2$. Compute $g_i = \frac{\hat{v}_i - \hat{v}_{i-1}}{\hat{x}_i - \hat{x}_{i-1}}$ and $g_{i+1} = \frac{\hat{v}_{i+1} - \hat{v}_i}{\hat{x}_{i+1} - \hat{x}_i}$.
5. If $|\frac{\hat{x}'_{i+1} - x'_i}{\hat{x}_{i+1} - \hat{x}_i}| > \bar{M}$ and a right turn is made ($g_{i+1} < g_i$), then remove point $i+1$ from grids $\hat{\mathbb{X}}_t$, $\hat{\mathbb{V}}_t$ and $\hat{\mathbb{X}}'_t$. Otherwise, set $i = i + 1$.
6. If $i + 1 \leq |\hat{\mathbb{X}}_t|$, then repeat from step 5.

Note that the 'jump detection' threshold $\bar{M}$ arises naturally in economic problems since the maximum curvature of a policy function *conditional on a sequence of future discrete choices* is bounded above as marginal propensities to save are also bounded above (White, 2015; Carroll, 2023). Thus, $\bar{M}$ can either be set to the maximum marginal propensity to save, or it can also be analytically evaluated for each grid point (see Appendix A).

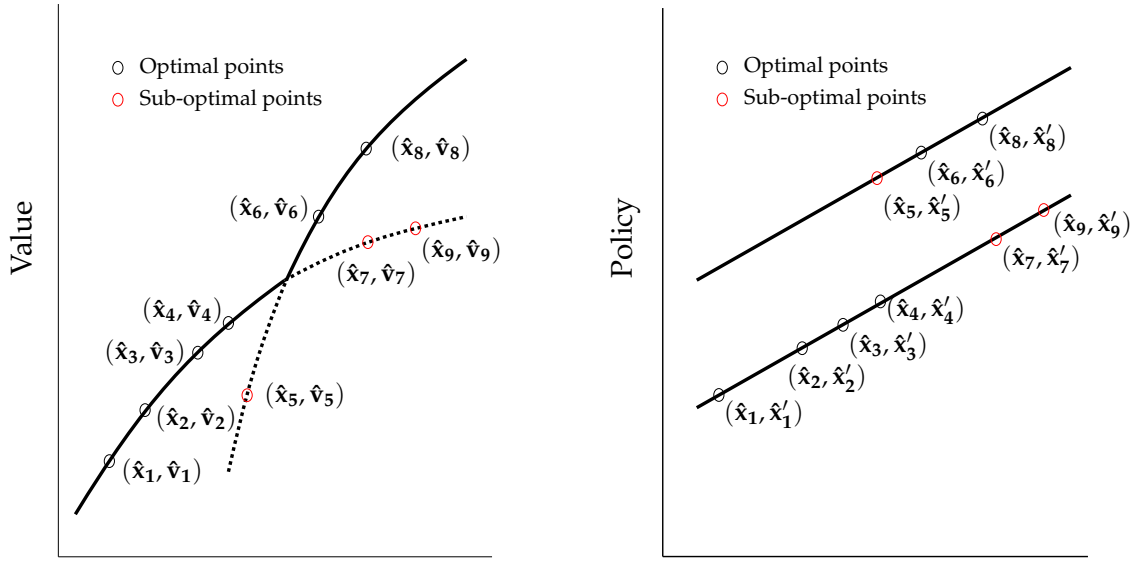

Figure 2: FUES eliminates points that cause a concave 'right turn' (left panel) from an optimal point and also cause a discontinuous jump in policy (right panel).

The method will thus yield a set of refined grids $\mathbb{X}_t$, $\mathbb{V}_t$ and $\mathbb{X}'_t$. To address the occasionally binding financial assets constraint $a_{t+1} \geq 0$, we follow the inverse Euler equation approach formalized by Dobrescu and Shanker (2024). In particular, we construct a constrained region of solution points as an array of consumption values c_t^1 such that $u'(c_t^1) > \beta(1+r)u'(c')$, where c' is next period consumption if $a' = 0$. The constrained region can then be appended to the unconstrained endogenous grid to create a single endogenous grid. The policy and value functions can then be interpolated over these grids to yield the time t approximated solution for the worker who chooses to continue working. The retiree value and policy functions can be calculated using standard EGM since the retiree problem is concave at each time t. Once the retiree problem is solved for time t, the discrete choice at time t of whether or not to work at time $t+1$ can be evaluated. The procedure can then be repeated at $t-1$ as per standard backward policy iteration.

2.1.4 Forward and backward scans and crossing points

So far, we assumed that if a point $(\hat{x}_{i+1}, \hat{v}_{i+1})$ makes a left turn from point $(\hat{x}_i, \hat{v}_i)$, then it is a sufficient and *necessary* condition for the point $(\hat{x}_{i+1}, \hat{v}_{i+1})$ to lie after a crossing point of two value functions between itself and $(\hat{x}_i, \hat{v}_i)$. However, a point $(\hat{x}_{i+1}, \hat{v}_{i+1})$ may lie after such a crossing point and yet not generate a left turn with respect to point x_i - see the left panel of Figure 3. We also assumed that the first point after a crossing point $(\hat{x}_{i+1}, \hat{v}_{i+1})$

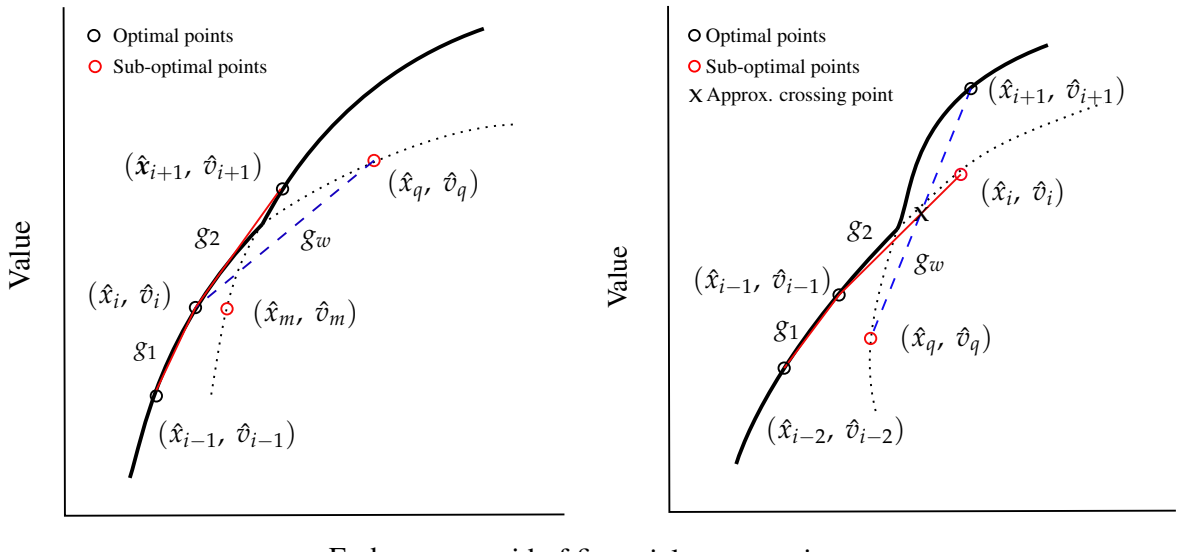

Figure 3: Forward and backward scans to improve accuracy of FUES around crossing points.

must be on the optimal choice-specific value function. However, a selected point may be the first point after a crossing between choice-specific value functions and yet not be optimal - see the right panel of Figure 3 where the point $(\hat{x}_i, \hat{v}_i)$ is sub-optimal but will not be removed by the basic FUES method since it is on the same sequence of future discrete choices as the optimal point right before the crossing. To rectify the issue in the left panel of Figure 3, we can implement a forward scan before a point is eliminated. A forward scan picks a point $\hat{x}_q$ to the right of $\hat{x}_{i+1}$ that is on the same value function as $\hat{x}_i$. The point $\hat{x}_q$ can be found by checking points after $i+1$ in the endogenous grid and finding the first point whose policy function does not jump from the point $\hat{x}_i$. We can then check to see if point $\hat{x}_{i+1}$ dominates the segment joining $(\hat{x}_i, \hat{v}_i)$ to $(\hat{x}_q, \hat{v}_q)$, drawn as g_w in the left panel of Figure 3. If $\hat{x}_{i+1}$ dominates the segment, it means $\hat{x}_{i+1}$ lies after a crossing point and must be included as an optimal point.

To rectify the issue in the right panel of Figure 3, we can implement a backward scan after making a left turn. A backward scan picks a point $\hat{x}_q$ to the left of $\hat{x}_i$ that is on the same value function as $\hat{x}_{i+1}$. The point $\hat{x}_q$ can be found by checking points before i in the endogenous grid and finding the first point whose policy function does not jump from the point $\hat{x}_{i+1}$. We can then check to see if point $\hat{x}_i$ is dominated by the segment joining $(\hat{x}_{i+1}, \hat{v}_{i+1})$ to $(\hat{x}_q, \hat{v}_q)$, drawn as g_w in the right panel of Figure 3. If $\hat{x}_i$ is dominated by the segment, it means $\hat{x}_i$ lies after a crossing and must not be included as an optimal point.

Finally, note that the forward and backward scan procedures can be used to attach ap-

proximations of the choice-specific value function crossing points to the endogenous grid. For instance, in the right panel of Figure 3, a crossing point can be attached at the intersection of the segment g_w with the segment g_2.

2.1.5 Numerical implementation

We apply our method to solve the model studied in Iskhakov et al. (2017), with Figure 4 showing how FUES removes sub-optimal points in the value function (left panel) and selects the optimal policy function (right panel). (Figure 8 in the Appendix plots the policy functions for workers at different ages, as a direct comparison to Figure 3 in Iskhakov et al. (2017).) To compare numerical performance, we also compute the upper envelope using (i) RFC as in Dobrescu and Shanker (2024), and (ii) DC-EGM as in Iskhakov et al. (2017) using the code libraries provided by Carroll et al. (2018). Table 1 shows each method's speed and mean Euler error for different sizes of financial assets grid and utility costs δ. We see all three methods are comparable in terms of accuracy, though RFC and FUES are slightly more accurate than DC-EGM. However, FUES is significantly faster across all grid-sizes, being more than five (eight) times faster than DC-EGM (RFC) on average.

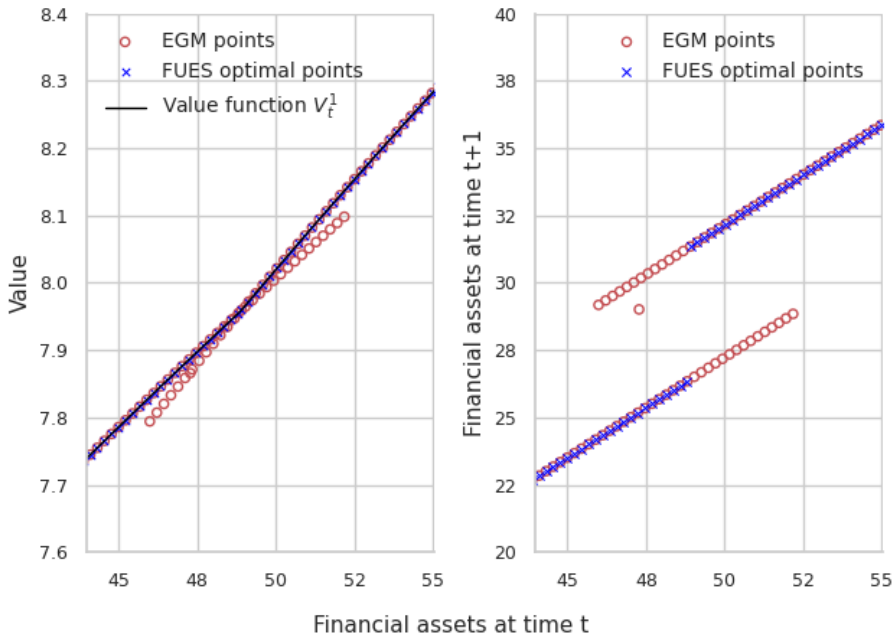

Figure 4: Value correspondence and optimal points for $t = 17$.

The speed gains arise from the lower FUES complexity. Compared to RFC, FUES does not require conducting a nearest neighbour search around each endogenous grid point.

Table 1: Speed and accuracy of FUES in the retirement choice model without taste shock.

Grid size	δ	*Upper envelope time*			*Euler error*		
		RFC	**FUES**	**DC-EGM**	**RFC**	**FUES**	**DC-EGM**
500	0.25	1.211	0.110	0.360	-1.537	-1.591	-1.537
	0.50	1.307	0.110	0.519	-1.557	-1.606	-1.556
	1.00	1.418	0.109	0.651	-1.634	-1.611	-1.634
1000	0.25	2.870	0.216	0.636	-1.537	-1.591	-1.537
	0.50	2.836	0.215	1.061	-1.556	-1.606	-1.556
	1.00	3.097	0.212	2.248	-1.630	-1.658	-1.629
2000	0.25	5.566	0.431	1.289	-1.537	-1.591	-1.537
	0.50	5.693	0.428	1.986	-1.556	-1.607	-1.557
	1.00	7.353	0.428	4.761	-1.629	-1.635	-1.629
3000	0.25	8.426	0.648	1.979	-1.537	-1.591	-1.537
	0.50	11.402	0.643	2.983	-1.557	-1.607	-1.557
	1.00	12.807	0.625	6.630	-1.629	-1.660	-1.629

Notes: Model parameters: $T = 50$, $\beta = 0.96$, $r = 0.02$, $y = 20$, and $a_t \in [0, 500]$. A 4-step forward and backward scan is used by FUES to refine the upper envelope. Upper envelope time is reported in milliseconds, while mean Euler error is reported in decimal logarithms (Judd, 1992; Fella, 2014; Druedahl and Jørgensen, 2017).

Additionally, FUES does not compare each possible combination of nearby grid points to determine whether one point is sub-optimal but tests whether a point is sub-optimal by comparing only to an adjacent point already the upper envelope. Compared to DC-EGM, FUES performs a single scan and does not require a separate interpolation step over multiple monotone segments.

The performance of FUES is also consistent across different values of the utility cost δ, while the performance of DC-EGM tends to vary. The reason δ affects the performance of DC-EGM is that the endogenous grid points may not always generate discernible increasing monotone segments but rather also form smaller decreasing segments or isolated points; this can occur either due to interpolation errors in the next period policy function, or due to the presence of uncertainty. With added isolated points and smaller segments, DC-EGM needs to compare additional interpolants to determine the upper envelope. As the endogenous grid becomes irregular due to variation in parameter values or uncertainty, the number of interpolants DC-EGM has to construct can grow arbitrarily large.

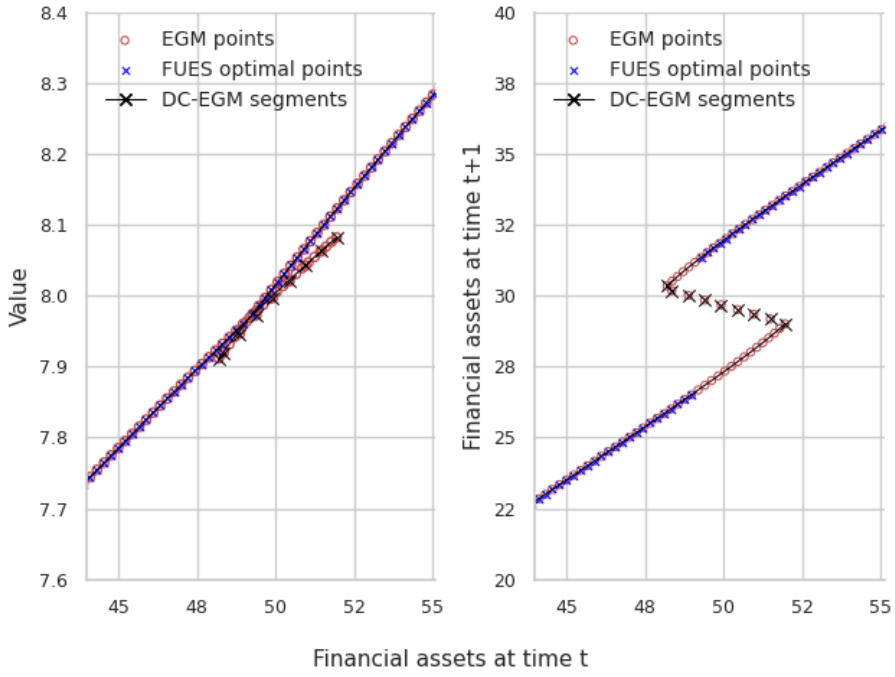

Figure 5: Non-monotone endogenous grid points in presence of taste shocks.

Table 2: Speed and accuracy of FUES in the retirement choice model with taste shock.

Grid size	δ	*Upper envelope time*			*Euler error*		
		RFC	**FUES**	**DC-EGM**	**RFC**	**FUES**	**DC-EGM**
500	0.25	1.536	0.110	1.091	-1.164	-1.194	-1.172
	0.50	1.406	0.109	1.206	-1.185	-1.222	-1.181
	1.00	1.413	0.106	0.926	-1.399	-1.353	-1.392
1000	0.25	3.063	0.212	2.062	-1.132	-1.194	-1.166
	0.50	3.204	0.214	2.161	-1.170	-1.218	-1.190
	1.00	2.772	0.213	1.833	-1.416	-1.312	-1.380
2000	0.25	6.209	0.422	4.375	-1.127	-1.195	-1.162
	0.50	6.701	0.422	4.238	-1.165	-1.215	-1.191
	1.00	6.431	0.421	3.484	-1.418	-1.308	-1.380
3000	0.25	10.876	0.642	7.079	-1.126	-1.195	-1.151
	0.50	12.815	0.638	6.979	-1.176	-1.216	-1.195
	1.00	12.825	0.648	4.987	-1.408	-1.286	-1.380

Notes: Model parameters: $T = 50$, $\beta = 0.96$, $r = 0.02$, $y = 20$, $\bar{s} = 0.05$, and $a_t \in [0, 500]$. A 4-step forward and backward scan is used by FUES to refine the upper-envelope. Upper envelope time is reported in milliseconds, while mean Euler error is reported in decimal logarithms (Judd, 1992; Fella, 2014; Druedahl and Jørgensen, 2017).

To further illustrate the ability of FUES to robustly handle more complex endogenous grids with non-monotone segments and isolated points, we also compare the performance of FUES and DC-EGM in a model where an extreme value taste shock with scale parameter $\bar{s}$ is added to the utility of workers (see Iskhakov et al. (2017) for details of the model with taste shocks). The resulting endogenous grid is illustrated in Figure 5, where decreasing non-monotone parts of the endogenous grid lead to a significant number of additional segments the DC-EGM algorithm has to process. The presence of these smaller segments leads to slower performance for DC-EGM (see Table 2), with FUES now close to an order of magnitude faster than DC-EGM, while still maintaining its higher accuracy.

2.2 Application 2: Continuous housing investment with frictions

Having introduced FUES via a simple application, we now turn to demonstrate it in a housing frictions model where the DC-EGM method fails due to the non-monotonicity of the policy function. Interestingly, this model features two dimensions of savings, one for liquid (financial) assets and one for illiquid (housing) assets. Despite being a veritable workhorse in the housing frictions literature (Kaplan and Violante, 2014; Yogo, 2016; Dobrescu et al., 2024), the conditions that Iskhakov (2015) requires for multidimensional 'pure EGM' do not hold here, with the set of Euler equations not analytically invertible. This example thus also shows how one-dimensional EGM and FUES can be practically applied to a multidimensional setting where 'pure EGM' fails. The solution strategy will involve numerically obtaining all the roots of the financial assets Euler equation along a single dimension, and then evaluate the optimal non-monotonic housing policy, and implicitly the optimal financial assets policy, using EGM and FUES.

2.2.1 Model environment

Let non-negative liquid (financial) assets be denoted by a_t, and non-negative housing assets be denoted by H_t. Consider financial assets earn a rate of return r, and assume for simplicity that housing earns no returns. Investments can be made in and out of the stock of a_t without friction, while adjusting housing to a value H_{t+1} requires a payment of τH_{t+1}, with $\tau > 0$. In each period t, with $t = 0, 1 \ldots, T$, the agent consumes non-housing goods c_t, and invests a total of H_{t+1} and a_{t+1} in housing and financial assets, respectively. The agent also makes a discrete choice d_t, where investment in and out of housing assets can only be made if $d_t = 1$; otherwise if $d_t = 0$ then $H_{t+1} = H_t$. Finally, in each period, the agent earns a stochastic wage y_t and we assume $(y_t)_{t=0}^{T}$ is a finite, Markov process.

The following constraints will hold for each t: first, total investments and consumption cannot exceed total available wealth each period,

$$(1+r)a_t + y_t + d_t H_t \geq a_{t+1} + c_t + d_t(1+\tau)H_{t+1}, \tag{12}$$

where total wealth at time t is denoted by $x_t = (1+r)a_t + y_t + d_t H_t$.

Second, in terms of payoffs, the agent lives up to time T, after which they die and value the bequest they leave behind according to a function $\theta\colon \mathbb{R}_+ \to \mathbb{R} \cup \{-\infty\}$. Per-period utility is given by a real-valued function $\varphi_t^u\colon \mathbb{R}_+ \times \mathbb{R}_+ \to \mathbb{R} \cup \{-\infty\}$ defined as

$$\varphi_t^u(c_t, H_{t+1}) = \mathbb{1}_{t\leq T} u(c_t, H_{t+1}) + \mathbb{1}_{t=T+1}\theta(c_{T+1}), \tag{13}$$

where u is a concave, jointly differentiable, increasing function of non-housing consumption c_t and end-of-period housing H_{t+1} (Yogo, 2016). Formally, the agent's dynamic optimization problem becomes

$$V_0(a_0, H_0, y_0) = \max_{(a_t, H_t, d_t)_{t=0}^{T+1}} \sum_{t=0}^{T+1} \beta^t \mathbb{E}\varphi_t^u(c_t, H_{t+1}), \tag{14}$$

such that (12) and (13) hold, $H_t \geq 0$ and $a_t \geq 0$ for each t, a_0, H_0 and y_0 are given, and the expectation is taken over the wage process $(y_t)_{t=0}^T$. The sequential problem implies the following recursive Bellman equation:

$$V_t(a, H, y) = \max_{a', H', d} \left\{\varphi_t^u(c, H') + \beta \mathbb{E}_y V_{t+1}(a', H', y')\right\}, \tag{15}$$

where the prime notation indicates next period state values satisfying the budget constraint (12), $c = y_t + (1+r)a + dH - a' - d(1+\tau)H'$, and expectations are now conditional on the realization y of the time t wage y_t.

2.2.2 The Euler equations

The problem will feature two Euler equations, one for each state. For periods prior to the terminal one, the Euler equation for the financial assets is

$$u_1(c_t, H_{t+1}) \geq \beta(1+r)\mathbb{E}_t u_1(c_{t+1}, H_{t+2}), \tag{16}$$

where we have used the subscript '1' to refer to the first partial derivative of u, and will use the subscript '2' to refer to the second partial derivative of u. If $d_t = 1$, the Euler

equation for housing is

$$(1+\tau)u_1(c_t, H_{t+1}) \geq \overbrace{\mathbb{E}_t \sum_{k=t}^{\iota-1} \beta^{t-\iota} u_2(c_k, H_{k+1})}^{\text{Marginal value of housing services stream}} + \underbrace{\mathbb{E}_t \beta^{t-\iota} \left(u_1(c_\iota, H_{\iota+1})\right)}_{\text{Marginal value of liquidating housing at time } \iota} . \tag{17}$$

The intuition of the Euler equation (16) for financial assets is standard. The Euler equation for housing (17), however, features a stochastic time subscript ι, defined as the next period when $d_\iota = 1$. Since the next time housing is adjusted will be stochastic, ι becomes a random stopping time. The Euler equation for housing then tells us that the shadow value (price) of investment (or withdrawal) from the stock of housing assets is given by the discounted expected value of housing *when housing is next liquidated*, along with the stream of housing services provided up to the time of liquidation.

Functional Euler equations. Since the solution sequence for the problem is recursive, there exists measurable functions σ_t^a, σ_t^H and $\mathcal{I}_t$ such that $H_{t+1} = \sigma_t^H(a_t, H_t, y_t)$, $a_{t+1} = \sigma_t^a(a_t, H_t, y_t)$ and $d_t = \mathcal{I}_t(a_t, H_t, y_t)$ for each t. Let $\sigma_t^{a,d}$ and $\sigma_t^{H,d}$ be the choice-specific policy functions conditional on the time t discrete choice $d \in \{0, 1\}$. Inserting the policy functions back into (16) - (17) yields the following functional Euler equation for housing:

$$\begin{aligned} u_1(c, H')(1+\tau) \geq \beta \mathbb{E}_y \mathcal{I}_{t+1}(a', H', y') u_1(c', H'') + u_2(c, H') \\ + (1 - \mathcal{I}_{t+1}(a', H', y'))\beta \left[\mathbb{E}_y \Theta_{t+1}(a', H', y') + u_2(c', H')\right], \end{aligned} \tag{18}$$

where we have that

$$\begin{aligned} c' = (1+r)\sigma_t^{a,1}(a, H, y) + \sigma_t^{H,1}(a, H, y) + y' \\ - \sigma_{t+1}^{a,1}(a', H', y') - \sigma_{t+1}^{H,1}(a', H', y')(1+\tau), \end{aligned} \tag{19}$$

$$c = (1+r)a + H + y - \sigma_t^{a,1}(a, H, y) - \sigma_t^{H,1}(a, H, y)(1+\tau), \tag{20}$$

$$H'' = \sigma_{t+1}^{H,1}(a', H', y), \tag{21}$$

$a' = \sigma_t^{a,1}(a, H, y)$, $H' = \sigma_t^{H,1}(a, H, y)$, and Θ_{t+1} is a multiplier denoting the continuation marginal value of housing if time $t+1$ housing stock is not adjusted. For a set of time

$t+1$ recursive policy functions, we can compute Θ_t as a function of the states as follows:

$$\Theta_t(a, H, y) = \mathbb{E}_y \mathcal{I}_{t+1}(a', H', y') + u_2(c, H') \\ + \beta \mathbb{E}_y (1 - \mathcal{I}_{t+1}(a', H', y')) \left[\Theta_{t+1}(a', H', y') + u_2(c', H') \right]. \quad (22)$$

The functional Euler equation for the liquid assets then becomes

$$u_1(c, H') \geq \beta(1+r)\mathbb{E}_y u_1(c', H''), \quad (23)$$

with c, c' H' defined analogously to (19) and (20), and where if the time t discrete choice is not to adjust, then $d = 0$.

2.2.3 Computation using EGM and FUES

Suppose we know V_{t+1}, $\{\sigma_{t+1}^{a,d}, \sigma_{t+1}^{H,d}\}_{d \in \{0,1\}}$, $\mathcal{I}_{t+1}$ and Θ_{t+1}. We can first apply standard EGM with FUES to evaluate $\sigma_t^{a,0}$ for non-adjusters since only one Euler equation (i.e., equation (23)) will hold. For each possible time t housing state H_t in the housing grid and exogenous state y_t, we can approximate $\sigma_t^{a,0}(\cdot, H_t, y_t)$ by first setting an exogenous grid of a' values (holding $H' = H_t$ fixed since no adjustment takes place), and then creating an endogenous grid of time t financial assets using (23) and (12). FUES can then be applied as in Section 2.1.3 to eliminate sub-optimal points, allowing us to obtain an approximation of the policy function $\sigma_t^{a,0}$.[1]

Let us now calculate the housing policy functions for adjusters. First, note we can evaluate consumption today c, for a given value of H' and a', as

$$c = u_1^{-1}((1+r)\beta \mathbb{E}_y u_1(c', H''), H'), \quad (24)$$

where u_1^{-1} is the analytical inverse of u_1 in its first argument. We evaluate the policy functions for adjusters is as follows:

[1] To address occasionally binding constraints, we follow the approach in Dobrescu and Shanker (2024).

Box 2: FUES and EGM for adjuster policy function

1. Fix y, fix an exogenous grid $\tilde{\mathbb{H}}'$ over H', and initialise empty arrays for the housing policy ($\hat{\mathbb{H}}'$), value correspondence ($\hat{\mathbb{V}}$), financial assets policy function ($\hat{\mathbb{A}}'$), and endogenous wealth grid ($\hat{\mathbb{X}}$).
2. For each $\hat{h}_i \in \tilde{\mathbb{H}}'$:
   (i) Evaluate the P multiple roots to (18) in terms of a', with c evaluated by (24) and H' fixed as $\hat{h}_i$; collect the roots in a tuple $(\hat{a}'^{,0}, \ldots, \hat{a}'^{,p}, \ldots \hat{a}'^{,P})$.
   (ii) For each root in $(\hat{a}'^{,0}, \ldots, \hat{a}'^{,p}, \ldots, \hat{a}'^{,P})$, evaluate the endogenous grid points of wealth $(\hat{x}^0, \ldots, \hat{x}^p, \ldots, \hat{x}^P)$ using the budget constraint[a]

$$\hat{x}^p = \hat{a}'^{,p} + (1+\tau)\hat{h}_i + c,$$

   and evaluate the current period values $(\hat{v}'^{,0}, \ldots, \hat{v}'^{,p}, \ldots \hat{v}'^{,P})$ as

$$\hat{v}'^{,p} = u(c, \hat{h}_i) + \mathbb{E}_y V_{t+1}(\hat{a}'^{,p}, \hat{h}_i).$$

   (iii) Append the P multiple roots $(\hat{a}'^{,0}, \ldots, \hat{a}'^{,p}, \ldots \hat{a}'^{,P})$ to $\hat{\mathbb{A}}'$, the time t values to $\hat{\mathbb{V}}$, the endogenous grid points to $\hat{\mathbb{X}}$, and P copies of $\hat{h}_i$ to $\hat{\mathbb{H}}'$.
3. Apply FUES (Box 1, Section 2.1.3) to the grids $\hat{\mathbb{V}}$, $\hat{\mathbb{X}}$ and $\hat{\mathbb{H}}$ to recover the refined endogenous grid points $\mathbb{X}$, value grid $\mathbb{V}$, and policy grids $\mathbb{A}'$ and $\mathbb{H}'$.

[a] To save computation time, the endogenous grid for adjusters is defined in terms of total wealth x, where $x = (1+r)a + y + H$ since once housing is liquidated, only total wealth will affect the agent's decision.

We can apply the above steps to each y in the exogenous shock grid. With $\sigma_t^{H,1}$ and $\sigma_t^{a,1}$ approximated on a uniform grid, we can then construct σ_t^H and σ_t^a in the standard way, by comparing the value function for adjusters and non-adjusters at each point on the uniform grid of current period states.

Before we turn to the numerical example, let us discuss how the non-monotonicity of the endogenous grid points arises for the housing-adjusting policy functions. The EGM above generates an exogenous grid $\hat{\mathbb{H}}'$ and an endogenous grid $\hat{\mathbb{X}}$ that satisfy

$$\begin{aligned} u_1(\hat{c}, \hat{H}') = {} & \beta \mathbb{E}_y \mathcal{I}_{t+1}(\hat{\psi}_t(\hat{x}, \hat{H}'), \hat{H}', y') u_1(c', H'') + u_2(c, H') \\ & + (1 - \mathcal{I}_{t+1}(\hat{\psi}_t(\hat{x}, \hat{H}'), \hat{H}', y')) \beta \mathbb{E}_y \left[\Theta_{t+1}(\hat{\psi}_t(\hat{x}, \hat{H}'), \hat{H}', y') + u_2(c', H') \right], \end{aligned} \quad (25)$$

where

$$\hat{c} = \hat{x} - \hat{\psi}_t(\hat{x}, \hat{H}') - (1+\tau)\hat{H}', \tag{26}$$

and c' and H'' defined as in (19) - (21). The function $\hat{\psi}_t$ gives the value of a' that satisfies the financial asset Euler equation (23), for a given value of $\hat{x}$ and $\hat{H}'$. To see the source of the non-monotoncity of H' in terms of the $\hat{x}$ above, first note how holding $\hat{\psi}_t$ fixed, the term on the LHS of (25) falls as wealth $\hat{x}$ increases, resulting in a higher level of housing investment. However, allowing $\hat{\psi}_t$ to also adjust alongside $\hat{x}$ implies that $\hat{\psi}_t$ may experience a discontinuous jump up, causing a discontinuous rise in the marginal utility of consumption today and a discontinuous *fall* in housing investment. Such a discontinuous jump in $\hat{\psi}_t$ occurs because $\hat{\psi}_t$ is not evaluated for a fixed future path of discrete choices. If the agent reaches in the future a certain level of wealth and upgrades their stock of housing, they will discontinuously decrease their non-housing consumption, causing a jump in the RHS of (23).[2]

2.2.4 Numerical implementation

To parameterize the model, we use the following separable specification for non-housing consumption and housing:[3]

$$u(c, H) = \frac{c^{\gamma-1} - 1}{\gamma - 1} + \alpha \log(H), \tag{27}$$

and define bequests as $\theta(c) = \bar{\theta} u(c, 0)$. For simplicity, we assume i.i.d. wage shocks with a random variable $\tilde{z}$ taking values in $[0.1, 1]$ with equal probability, and assume $y_t = \tilde{y}t(\tilde{z})$ where $\tilde{y}t$ is the wage function for females in Dobrescu et al. (2016).

Since the exogenous grid is irregular, with no clearly discernible monotone segments, DC-EGM cannot be applied. However, both FUES and RFC can be used to recover the upper envelope of the points recovered from inverting the Euler equation on the exogenous grid. Thus, we benchmark FUES against RFC (Dobrescu and Shanker, 2024) and NEGM (Druedahl, 2021). NEGM first approximates the non-adjuster policy function evaluated using EGM and DC-EGM, then solves the adjuster problem using VFI. [4]

[2] In terms of the monotone comparative static arguments given by Iskhakov et al. (2017) in Theorem 4., allowing a' to adjust implicitly as a function H' implies that the continuation value no longer enjoys the single crossing property since now the per-period payoff u also exhibits a jump and is not concave.

[3] Implementation using a non-seperable utility function is demonstrated in the FUES online repository.

[4] Since the non-adjuster policy function is monotone given H', DC-EGM can be applied to the nested non-adjuster problem. We implement the numerical optimization for NEGM using a combination of Nelder-Mead and Brent's method.

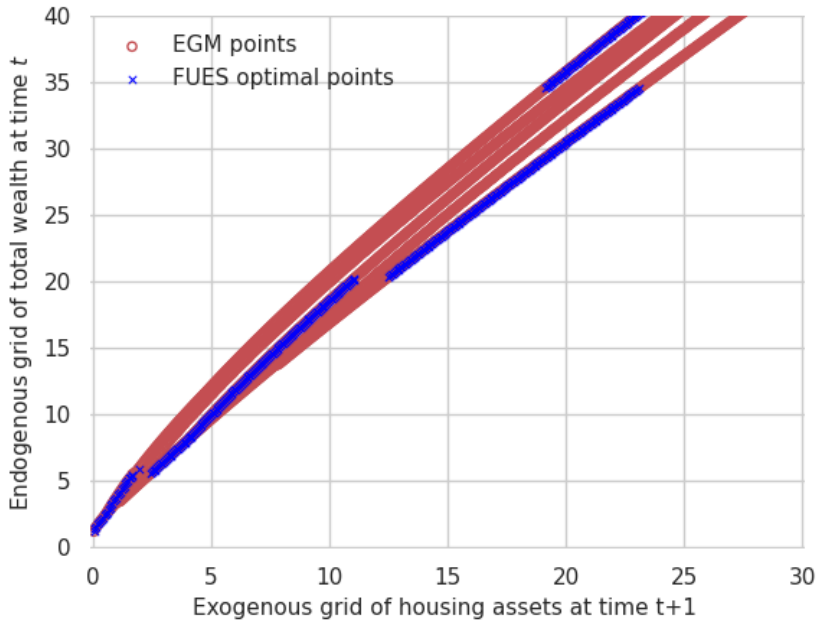

Figure 6: EGM total wealth points plotted on a uniform exogenous grid in the housing model with frictions.

The map of endogenous grid points to the exogenous grid $\hat{\mathbb{H}}'$ for a 59-year-old is shown in Figure 6. (Figure 9 in the Appendix further compares policy functions computed via NEGM with those computed via FUES and EGM.) First, note that there are multiple endogenous grid points for each value of the exogenous grid. Second, the endogenous grid has no discernible monotone segments that can be identified by the DC-EGM as in Iskhakov et al. (2017). Third, the optimal endogenous grid 'jumps down', implying the policy function is not monotone. By zooming in on the top right section of the exogenous grid in Figure 7 we can see, however, how FUES successfully recovers the optimal solution points by eliminating all jumps in the policy function that do not result in a left turn on the value function.

The numerical performance of FUES is shown in Table 3 for different sizes of housing and financial assets grid and transaction costs τ. Since NEGM does not include an upper envelope step that can be directly compared to FUES, Table 3 compares total iteration times for each solution method. Despite the root-finding operations performed by FUES, FUES is approximately 50% faster than NEGM. Notably, FUES achieves an order of magnitude improvement in accuracy over NEGM on average. The performance of FUES also remains consistent across various grid sizes and τ values.

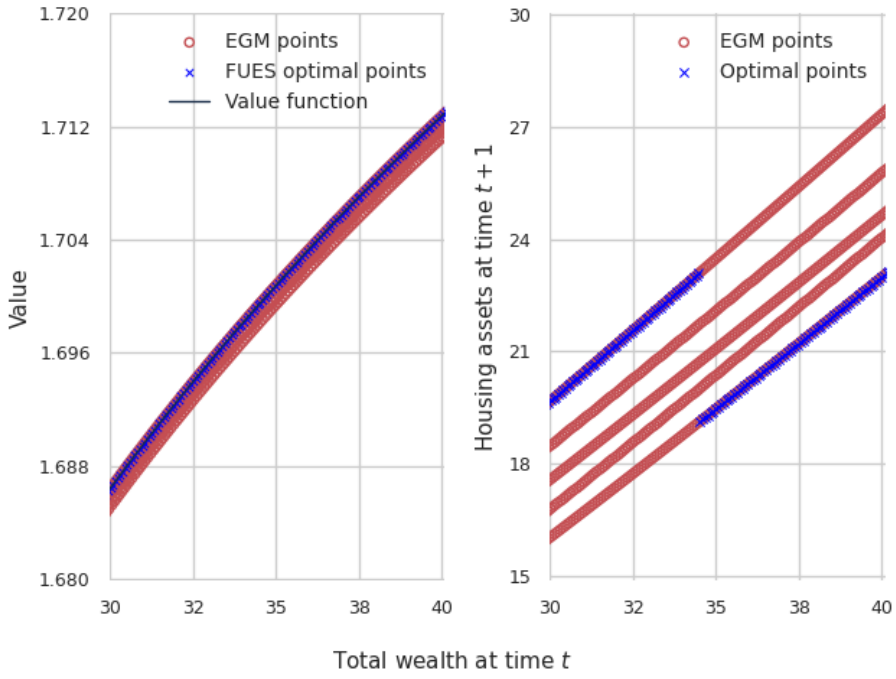

Figure 7: Value function and optimal housing policy function for the top right section of the endogenous grid in Figure 6.

As an additional performance test, we also compute an infinite horizon version of the housing frictions model with a stationary wage process. We solve the agent's problem using backward induction until the value function errors converge to a predefined tolerance level. Table 5 in the Appendix shows that FUES maintains a similar order of magnitude gain in accuracy over NEGM. Interestingly, this better FUES accuracy coming from eliminating the numerical optimization step also resulted in an average of 20% fewer iterations required to achieve convergence of the value function.

2.3 Application 3: Infinite horizon discrete housing choice model

We now turn to the discrete choice model of housing decisions in Fella (2014) where the housing choice grid itself is discrete. This application thus highlights the FUES robustness when there are a large number of discrete choices within each period.

2.3.1 Model environment

Consider an agent who draws an infinite sequence of bounded, stationary Markov wage shocks $(y_t)_{t=0}^{\infty}$. Each period the agent decides how much to consume of non-durable goods c_t, how much to save in liquid (financial) assets a_{t+1}, and how much to save in

Table 3: Speed and accuracy of FUES in the continuous housing investment with adjustment frictions model.

Grid Size	τ	*Time per iteration*			*Euler error*		
		RFC	**FUES**	**NEGM**	**RFC**	**FUES**	**NEGM**
250	0.03	5.414	5.043	7.608	-3.270	-3.183	-1.966
	0.07	5.425	4.844	7.617	-2.861	-2.819	-1.806
	0.15	5.380	4.757	7.653	-2.220	-2.194	-1.479
500	0.03	21.527	19.279	30.489	-3.265	-3.178	-2.067
	0.07	21.437	19.237	30.907	-2.855	-2.806	-1.934
	0.15	21.651	19.263	30.254	-2.234	-2.184	-1.576
1000	0.03	87.079	80.862	123.903	-3.259	-3.192	-2.170
	0.07	86.752	77.850	126.182	-2.843	-2.795	-2.038
	0.15	86.463	78.644	153.634	-2.222	-2.188	-1.648

Notes: Model parameters: $t_0 = 20$, $T = 60$, $\gamma = 3$, $\alpha = 0.66$, $\beta = 0.93$, $\tau = 0.12$, $r = 0.01$, $\bar{\theta} = 1.34$, $a_t \in [0, 20]$, and $H_t \in [0, 50]$. FUES jump detection threshold is $\bar{M} = 1.2$, with a 4-step forward and backward scan used. RFC jump detection threshold is $\bar{M} = 1.2$, with a search radius of 0.75. Time per iteration is reported in seconds, while mean Euler error is reported in decimal logarithms (Judd, 1992; Fella, 2014; Druedahl and Jørgensen, 2017).

housing assets H_{t+1}. Similar to Application 2, housing assets serve a dual role, namely they are a form of investment good but also provide durable consumption services. Moreover, housing can only be purchased in discrete amounts on a finite grid $\mathbb{H}$, and adjusting housing each period incurs a fixed transaction cost τH_{t+1}, with $\tau \in [0, 1)$. We assume no borrowing and so, $a_t \geq 0$ must hold.

Formally, the budget constraint is

$$a_{t+1} = (1 + r)a_t + y_t - (H_{t+1} - H_t) - \tau \mathbb{1}_{H_{t+1} \neq H_t} H_{t+1} - c_t, \tag{28}$$

with the per-period utility function defined by

$$u(c, H) = \alpha \log(c) + (1 - \alpha) \log(\kappa(H + \iota)), \qquad \kappa > 0, \iota > 0. \tag{29}$$

The agent's maximization problem yields the following value function:

$$V_0(a, y, H) = \max_{(a_t, H_t)_{t=0}^{\infty}} \mathbb{E} \sum_{t=0}^{\infty} \beta^t u(c_t, H_{t+1}), \tag{30}$$

such that (28) and (29) hold, $H_t \in \mathbb{H}$ and $a_t \geq 0$ for each t, and $a_0, y_0, h_0 = a, y, H$. Bellman

equation is thus

$$V(a, y, H) = \max_{c, H'} \left\{ u(c, H') + \mathbb{E}_y V'(a', y', H') \right\}, \tag{31}$$

such that a' satisfies the feasibility condition $a' \geq 0$ and the budget constraint (28) holds. Since this is an infinite horizon problem, recall the fixed point to the Bellman equation yields the value function, and the maximizing correspondence yields the policy functions.

2.3.2 The Euler equations

Let us write down the necessary Euler equation. Consider time $t+1$ policy functions σ^a_{t+1} and σ^H_{t+1}, which map the time $t+1$ states (i.e., financial assets a_{t+1} and housing H_{t+1}) to time $t+2$ states. We then have $a_{t+2} = \sigma^a_{t+1}(a_{t+1}, H_{t+1})$ and $H_{t+2} = \sigma^H_{t+1}(a_{t+1}, H_{t+1})$. A necessary condition is for a_{t+1} to solve the Euler equation in terms of a' as follows:

$$\begin{aligned} &u'((1+r)a_t + y_t - \Phi(H_t, H_{t+1}) - a') \\ &\qquad \geq \mathbb{E}_{y_t}(1+r)\beta u'((1+r)a' + y_{t+1} - \Phi(H_{t+1}, H_{t+2}) - \sigma^a_{t+1}(a', H_{t+1})), \end{aligned} \tag{32}$$

where we let $\Phi(H_t, H_{t+1}) = (H_{t+1} - H_t) - \tau \mathbb{1}_{H_{t+1} \neq H_t} H_{t+1}$ to ease the notation.

Once again, to state the source of the non-concavity here, recall that the standard approach in concave models is to solve a', then approximate σ_t, σ_{t-1}, σ_{t-2} and so on until σ_t converges. However, in the case of discrete choices, even if the choices H_{t+1} and H_{t+2} are held fixed or calculated to maximize the value function, the difficulty arises when we try to compute the policy functions recursively. Given the time $t+1$ asset policy function σ^a_{t+1}, c_{t+1} may not be monotone and there may be multiple roots to the above equation in a' because σ^a_{t+1} has implicitly inherited discrete choices from future periods. As a result, we may implicitly select a sub-optimal discrete choice for periods after time $t+2$ and hence select a sub-optimal local turning point a'.

2.3.3 Computation using EGM and FUES

In light of our discussion in Section 2.1, the use of FUES to the application here is straightforward. To proceed with computation using EGM and FUES, we can start with an initial guess for the value function V_T and policy functions σ^a_T and σ^H_T. Since there is only one Euler equation, we can use EGM without any root-finding steps and calculate the one-dimensional endogenous grid for each H, H' choice fixed. We then follow the procedure in Section 2.1.3 to remove sub-optimal grid points and evaluate the discrete choice policy function. Once approximations of V_{T-1}, σ^a_{T-1} and σ^H_{T-1} are obtained, we continue to

iterate until $\|V_{T-i} - V_{T-i-1}\|_\infty < \epsilon$ for some pre-determined $\epsilon > 0$. We use the same parameters as Fella (2014), except we set the lower bound on assets to zero, and use a simple 3-state process for wage shocks. Figure 10 in the Appendix shows the asset policy functions for different beginning-of-period housing levels (but allowing the end-of-period housing choice H' to be endogenous). Once again, we see that FUES is able to successfully recover the optimal policy function.

Table 4: Speed and accuracy of FUES in the discrete housing choice model.

Grid size A	*Grid size H*	*Upper envelope time*			*Euler error*		
		RFC	**FUES**	**DC-EGM**	**RFC**	**FUES**	**DC-EGM**
500	5	2.004	0.494	1.232	-2.212	-2.238	-1.903
	10	2.013	0.506	1.392	-2.225	-1.969	-1.873
	15	2.164	0.505	1.438	-1.944	-2.193	-2.178
1000	5	4.393	0.996	2.872	-2.273	-2.251	-2.225
	10	3.924	1.006	2.657	-2.406	-2.295	-2.081
	15	3.889	0.918	2.665	-2.294	-2.285	-2.276
2000	5	9.212	1.805	5.188	-2.140	-2.369	-2.318
	10	10.434	2.140	6.124	-2.487	-2.538	-2.329
	15	9.269	2.034	5.611	-2.408	-2.369	-2.393
3000	5	14.086	2.859	8.060	-2.419	-2.366	-2.354
	10	14.786	2.491	6.229	-2.221	-2.448	-2.400
	15	14.696	3.178	9.969	-2.484	-2.427	-2.434

Notes: Model parameters: $\beta = 0.93$, $r = 0.034$, $\tau = 0.09$, $\alpha = 00.77$, $\kappa = 0.077$, $\iota = 0.01$, $a_t \in [0, 30]$, and $H_t \in [0, 5]$. FUES jump detection threshold is $\bar{M} = 1.2$, with a 4-step forward and backward scan used. RFC jump detection threshold is $\bar{M} = 1.2$, with a search radius of 0.75. Upper envelope time is reported in milliseconds, while mean Euler error is reported in decimal logarithms (Judd, 1992; Fella, 2014; Druedahl and Jørgensen, 2017).

Table 4 compares FUES with RFC and DC-EGM in the discrete housing choice model for different grid sizes of financial assets (A) and housing (H). Since we analytically invert the Euler equation to produce the endogenous grid, all methods have comparable accuracy, with FUES slightly more accurate than DC-EGM. However, FUES is on average close to four (three) times faster than RFC (DC-EGM). The reason behind the speed advantage of FUES over DC-EGM being reduced here compared to Section 2.1 is that the number of jumps in the stationary policy function is significantly lower in the discrete housing choice model (i.e., DC-EGM has to compare fewer monotone segments). Nonetheless, FUES performance remains more consistent than DC-EGM as we vary the housing grid size and increase the number of jumps in the policy function.

3 General formulation of FUES

We now formally define a general discrete-continuous optimization problem, apply the EGM and state the FUES method as a formal pseudo-code, providing an illustrative proof to show how FUES recovers the optimal endogenous grid points.

3.1 The general discrete-continuous optimization problem

Let the set $\mathbb{D}$ be a finite family of discrete choices, and let $\{G^d\}_{d\in\mathbb{D}}$ be a family of continuously differentiable, increasing and strictly concave functions indexed by the discrete choices. Assume that $G^d\colon S \times Z \to \mathbb{R} \cup \{-\infty\}$ for each d, with $S \subset \mathbb{R}$ and $Z \subset \mathbb{R}$, and that S and Z are compact. In the context of a dynamic programming problem, each element in the choice set $\mathbb{D}$ will be a future stochastic sequence of history-dependent choices (and not a single discrete choice at a given time). However, for simplicity, going forward we refer to each d as a discrete choice. The function G^d will be the maximand on the RHS of the Bellman operator, holding the discrete choice fixed. Now, consider maximizing the upper envelope U of the choice-specific functions wrt. a continuous choice variable z

$$V(x) = \max_{z\in Z} \quad U(x,z), \tag{33}$$

where

$$U(x,z) = \max_{d\in\mathbb{D}} \quad G^d(x,z), \tag{34}$$

such that x is fixed. Next, define $\mathcal{I}(x,z) = \arg\max_d G^d(x,z)$ as the optimal discrete choice holding the arguments of each G^d fixed. Also, define the optimal policy function as

$$\sigma(x) = \arg\max_{z} \quad U(x,z), \tag{35}$$

and the choice-specific policy function and choice-specific value function as

$$\sigma^d(x) = \arg\max_{z} \quad G^d(x,z), \qquad Q^d(x) = \max_{z} \quad G^d(x,z). \tag{36}$$

Finally, define a twice differentiable and invertible transition function $f\colon S \times Z \to S$ that maps the current period choice and state to next period state in a dynamic programming problem. We set x' to denote the next period state, where x' will obey $x' = f(x,z)$.

Note that the mapping between our discrete-continuous optimization problem as stated

above and the three applications we tackle is as follows:

Application 1, Section 2.1. Fix t and consider agents making a decision to continue work in time $t+1$. Each d, with $d \in \mathbb{D}$, corresponds to a future path of feasible discrete choices made from $t+1$ to T. Formally, we can write $\mathbb{D} = \{0,1\}^{T-t}$. The choice-specific payoff $G^d(x,z)$ corresponds to $u((1+r)x + y - z) + V^d_{t+1}(z)$, where x denotes financial assets, z is the choice of next period assets, and V^d_{t+1} is the value function for those who work in $t+1$ conditional on the future path of discrete choices made from $t+1$ to T.

Application 2, Section 2.2. Fix t, recall our discussion in Section 2.2.3 and consider those making a decision to adjust their housing at time t. Each d, with $d \in \mathbb{D}$, corresponds to a future history-dependent path of housing adjustment choices from $t+1$ to T. The choice-specific payoff G^d corresponds to

$$G^d(x,z) = u(x - \hat{\psi}^d_t(x,z) - (1+\tau)z, z) + \mathbb{E}_{y_t} V^d_{t+1}(\hat{\psi}^d_t(x,z), z, y'),$$

where x is the total (financial and housing) wealth, z represents the $t+1$ housing choice, and V^d_{t+1} is the $t+1$ choice-specific value function. For a fixed discrete choice, the function $\hat{\psi}^d_t$ maps the wealth and housing choice to the optimal value of next period financial assets defined by the Euler equation (18).

Application 3, Section 2.3. Fix t and consider those making a decision to adjust housing at time t. Each d, with $d \in \mathbb{D}$, corresponds to an infinite history-dependent path of future housing choices. The choice-specific payoff G^d corresponds to the continuation payoff

$$G^d(x,z) = u((1+r)x + y_t + (1-\delta)H - z - (1+\tau)H', H') + \mathbb{E}_{y'} V^{d,\prime}(z, y'), \tag{37}$$

where z represents the next period financial assets choice, $V^{d,\prime}$ is the next period choice-specific value function, and H and H' are the fixed beginning- and end-of-period housing assets.

Since we have stated the above examples as reduced form dynamic programming problems, we have $x' = f(x,z) = z$.

3.1.1 The EGM and formal FUES pseudo-code

Let $\hat{\mathbb{X}}'$ be the exogenous grid of values x', with $|\hat{\mathbb{X}}'| = N$, where N is the exogenous grid size. We assume grids are sequences, that is $\hat{\mathbb{X}}' = \{\hat{x}'_0, \hat{x}'_1 \dots \hat{x}'_i \dots\}$. Recall that a necessary FOC for an interior solution to the discrete-continuous optimization problem is that $G_2^{\mathcal{I}(x,z)}(x,z) = 0$, where the subscript '2' denotes the partial derivative with respect

to the second argument of G^d. Also recall that if a continuous choice satisfies the FOC, it will be optimal conditional on the discrete choice (although, the discrete choice may not optimal). Formally:

Remark 1 *For $x \in S$, consider $\tilde{z}$ that satisfies $G_2^{\mathcal{I}(x,\tilde{z})}(x,\tilde{z}) = 0$. If $d = \mathcal{I}(x,\tilde{z})$ is fixed, then $\tilde{z}$ will satisfy $\tilde{z} = \arg\max_{z \in Z} G^d(x,z)$.*

We now define the unrefined endogenous grid of values $\hat{x}$ as

$$\hat{\mathbb{X}} \colon = \left\{ \hat{x} \in S \,\middle|\, \hat{x}' = f(\hat{x},z), G_2^{\mathcal{I}(\hat{x},z)}(\hat{x},z) = 0, \hat{x}' \in \mathbb{X}', z \in Z \right\}, \tag{38}$$

and we can also calculate unrefined grids containing candidate policies and values as

$$\hat{\mathbb{Z}} \colon = \left\{ \hat{z} \in Z \,\middle|\, \hat{x}' = f(x,\hat{z}), G_2^{\mathcal{I}(x,\hat{z})}(x,\hat{z}) = 0, \hat{x}' \in \mathbb{X}', x \in S \right\}, \tag{39}$$

$$\hat{\mathbb{V}} \colon = G^{\mathcal{I}(\hat{\mathbb{X}},\hat{\mathbb{Z}})}(\hat{\mathbb{X}}'). \tag{40}$$

Note the definition of the endogenous grid values above does not necessarily imply the values of $\hat{\mathbb{X}}$ can be calculated analytically. Rather, we leave open the possibility that the endogenous grid is a general grid (computed analytically or numerically) of points that satisfy the necessary FOCs of a discrete-continuous optimization problem.

The endogenous grid will be initially ordered in ascending order according to the order of $\hat{\mathbb{X}}'$. We then order the grids $\hat{\mathbb{X}}'$, $\hat{\mathbb{Z}}$, $\hat{\mathbb{V}}$, and $\hat{\mathbb{X}}$ by the values in $\hat{\mathbb{X}}$, and through a slight abuse of notation, continue to denote the reordered grids as $\hat{\mathbb{X}}'$, $\hat{\mathbb{Z}}$, $\hat{\mathbb{V}}$ and $\hat{\mathbb{X}}$. For each of these grids, the FUES method will generate a subsequence of refined grids $\mathbb{X}'$, $\mathbb{Z}$, $\mathbb{V}$ and $\mathbb{X}$ indexed by i_k, for instance, $\mathbb{X} = \{\hat{x}_0, \hat{x}_1, \ldots, \hat{x}_{i_k}, \ldots\}$. In the algorithm below, we let $N = |\hat{\mathbb{X}}|$ and $\bar{M}$ (i.e., the constant denoting the threshold at which FUES registers a jump between policy functions) be chosen by the researcher. Finally, $\mathcal{C}_{l+1}$ denotes a Boolean value that is true if point x_{l+1} is optimal, and $\mathcal{D}_l$ denotes a Boolean value that is true if x_k is not optimal and should be deleted.

Algorithm 1: Fast upper envelope scan

Data: $N > 0$, $\bar{M} > 0$, $\hat{\mathbb{X}}'$, $\hat{\mathbb{Z}}$,$\hat{\mathbb{V}}$,$\hat{\mathbb{X}}$
Result: $\mathbb{X}'$, $\mathbb{Z}$, $\mathbb{X}$ and $\mathbb{V}$

$k \leftarrow 1, l \leftarrow 1$;
$\hat{x}'_{i_q} \leftarrow \hat{x}'_q, \hat{v}_{i_q} \leftarrow \hat{v}_q, \hat{x}_{i_q} \leftarrow \hat{x}_q \quad q \leq 1$; /* Init. first two points. */
while $l < N$ **do**
  $g^v_k \leftarrow \frac{\hat{v}_{i_k} - \hat{v}_{i_{k-1}}}{\hat{x}_{i_k} - \hat{x}_{i_{k-1}}}, g^v_{l+1} \leftarrow \frac{\hat{v}_{l+1} - \hat{v}_{i_k}}{\hat{x}_{l+1} - \hat{x}_{i_k}}, g^x_{l+1} \leftarrow \frac{\hat{x}'_{l+1} - \hat{x}'_{i_k}}{\hat{x}_{l+1} - \hat{x}_{i_k}}$;
  if *If* $g^v_{l+1} \leq g^v_k$ *and* $|g^x_{l+1}| > \bar{M}$; /* Right turn, jump */
  then
    $\mathcal{C}_{l+1} \leftarrow$ False;
    $\mathcal{C}_{l+1} \leftarrow$ Forward scan ; /* Optional fwd. scan (Fig. 5) */
  else if $g^v_{l+1} > g^v_k$; /* Left turn */
  then
    $\mathcal{C}_{l+1} \leftarrow$ True ;
    $\mathcal{D}_l \leftarrow$ Backward scan ; /* Optional bwd. scan (Fig. 5) */
  else
    $\mathcal{C}_{l+1} \leftarrow$ True ; /* Right turn, no jump */
  end
  if $\mathcal{D}_l$ **then**
    $\hat{x}'_{i_k} \leftarrow \hat{x}'_{l+1}, \hat{v}_{i_k} \leftarrow \hat{v}_{l+1}$;
    $\hat{x}_{i_k} \leftarrow \hat{x}_{l+1}, \hat{z}_{i_k} \leftarrow \hat{z}_{l+1}$; /* Replace i_k sub-opt. point. */
  else if $\mathcal{C}_{l+1}$ **then**
    $\hat{x}'_{i_{k+1}} \leftarrow \hat{x}'_{l+1}, \hat{v}_{i_{k+1}} \leftarrow \hat{v}_{l+1}$;
    $\hat{x}_{i_{k+1}} \leftarrow \hat{x}_{l+1}, \hat{z}_{i_{k+1}} \leftarrow \hat{z}_{l+1}$; /* Add point; keep i_k opt. point. */
    $k = k + 1$
  else
    Pass
  end
  $l \leftarrow l + 1$;
end

3.2 Proving FUES recovers optimal points

3.2.1 Preliminaries and assumptions

The optimal subset of points $\mathbb{X}^\star$ of the endogenous grid can be defined as

$$\mathbb{X}^\star : = \left\{ \hat{x}_i \in \hat{\mathbb{X}} \,\middle|\, \hat{v}_i = V(\hat{x}_i) \right\}. \tag{41}$$

The following formalises the definition of the points on the space S where choice-specific value functions intersect:

Definition 1 *Let $T_P \subset S$ be the set of 'crossing points' between the choice-specific value functions. That is, the set of $x \in S$ such that for some $m, q \in \mathbb{D}$, $Q^m(x) = Q^q(x)$ and for some ϵ with $\epsilon > 0$, $V(x+\epsilon) = Q^q(x+\epsilon) > Q^m(x+\epsilon)$ and $V(x-\epsilon) = Q^m(x-\epsilon) > Q^q(x-\epsilon)$.*

In terms of required assumptions, we first assume that the distance between choice-specific policy functions is bounded below.

Assumption 1 *The term $|f(x, \sigma^d(x)) - f(x, \sigma^s(x))|$ is bounded below by a constant D for all $d, s \in \mathbb{D}$, $d \neq s$ and $x \in S$.*

Second, we assume that the rate of change of the next period states mapped by the transition and policy functions is uniformly bounded above by a common constant.

Assumption 2 *The family of functions $x \mapsto f(x, \sigma^d(x))$ for $d \in \mathbb{D}$ have a common Lipshitz constant M.*

Third and fourth, we also assume the distance between the endogenous grid points is small enough and the jump detection threshold is chosen such that FUES is able to use the previous assumptions to differentiate between a jump and a movement along a choice-specific policy function.

Assumption 3 *There exists $\delta > 0$ such that for all $x^\star_{j+1}, x^\star_j \in \mathbb{X}^\star$ we have $|x^\star_{j+1} - x^\star_j| \leq \delta$ and $\frac{D}{\delta} > 2M$.*

Assumption 4 *The jump detection threshold satisfies $\bar{M} \geq \frac{D}{\delta} - M$.*

Finally, we place some assumptions on the grid points around crossing points. The assumption below uses the notation from Definition 1 and says that the crossing points are included in the endogenous grid, and that the next period policy associated with a crossing point is associated with the choice-specific value function that 'crosses' the optimal value function from below.

Assumption 5 *We have $T_P \subset \mathbb{X}^\star$ and for each $\hat{x}_i \in \mathbb{X}^\star$ such that $\hat{x}_i \in T_P$, $\hat{x}'_i = f(\hat{x}_i, \sigma^m(\hat{x}_i))$.*

Next, we place conditions on the crossing points between choice-specific value functions. Item 1. states that the first point after a crossing is an optimal point, and item 2. states that an optimal point after a crossing is sufficiently close to the previous grid point to make a large enough left turn in the value function.

Assumption 6 *Fix $\tilde{x} \in T_P$ and let $x^\star_k$ be the largest element in $\mathbb{X}^\star$ such that $x^\star_k \leq \tilde{x}$ and $x^\star_{k+1}$ be*

the smallest element in $\mathbb{X}^\star$ such that $x^\star_{k+1} > \tilde{x}$. The following hold:

1. *We have $\hat{v}_{k+1} = Q^q(\hat{x}_{k+1})$ where Q^q is identified by Definition 1 as the value function crossing at point $\tilde{x}$ from below.*
2. *We have:*

$$\frac{Q^q(x^\star_{k+1}) - Q^q(x^\star_k)}{\delta} > \frac{Q^m(x^\star_{k+1}) - Q^q(x^\star_k)}{x^\star_{k+1} - x^\star_k} + \frac{Q^m(x^\star_k) - Q^m(x^\star_{k-1})}{x^\star_k - x^\star_{k-1}}. \tag{42}$$

3.2.2 Main result

Proposition 1 *Let Assumptions 1-6 hold and let $(\mathbb{X}, \mathbb{X}', \mathbb{Z}, \mathbb{V})$ be the tuple of outputs of Algorithm 1 without the forward and backward scans. If $\hat{v}_i = V(\hat{x}_i)$ for $i = 1, 2$, then $\mathbb{X} = \mathbb{X}^\star$.*

Proof. We can prove the proposition above by proving the following claim holds:

$$\hat{x}_i \in \mathbb{X} \iff \hat{x}_i \in \mathbb{X}^\star, \qquad i \leq l,\ \hat{x}_i \in \mathbb{X}, \tag{43}$$

for $l = |\mathbb{X}|$. We will show that if the claim holds for all i with $i \leq l$ for some l, then it will hold for all i with $i \leq l + 1$. Thus, by the principle of induction, the claim will hold for all i with $i \leq l$ for any l. In particular, the claim will hold for $l = |\mathbb{X}|$. As such, begin the proof by making the inductive assumption that the claim at (43) holds for all i with $i \leq l$ for some $l \leq |\mathbb{X}|$. Moreover, let $\{\hat{x}_{i_0}, \ldots, \hat{x}_{i_j}, \ldots, \hat{x}_{i_k}\}$ denote the first k points of the subsequence $\mathbb{X}$ such that i_k satisfies $i_k \leq l$.

Part 1: Proof that $\hat{x}_i \in \mathbb{X} \implies \hat{x}_i \in \mathbb{X}^\star$ holds for all i with $i \leq l + 1$.

If $i_{k+1} > l + 1$, then the proof of this part is complete since $\hat{x}_i \in \mathbb{X} \implies \hat{x}_i \in \mathbb{X}^\star$ continues to hold for all $i < l + 1$ by the inductive assumption. On the other hand, suppose $i_{k+1} = l + 1$ and the point $\hat{x}_{i_{k+1}}$ satisfies $\hat{x}_{i_{k+1}} \in \mathbb{X}$. There are two cases. The first case arises if a right turn is made on the value correspondence, $\frac{\hat{v}_{i_{k+1}} - \hat{v}_{i_k}}{\hat{x}_{i_{k+1}} - \hat{x}_{i_k}} \leq \frac{\hat{v}_{i_k} - \hat{v}_{i_{k-1}}}{x_{i_k} - \hat{x}_{i_{k-1}}}$. The second case arises if a left turn is made on the value correspondence, $\frac{\hat{v}_{i_{k+1}} - \hat{v}_{i_k}}{\hat{x}_{i_{k+1}} - \hat{x}_{i_k}} > \frac{\hat{v}_{i_k} - \hat{v}_{i_{k-1}}}{\hat{x}_{i_k} - \hat{x}_{i_{k-1}}}$.

[Part 1, Case I: Right turn]

Let $\frac{\hat{v}_{i_{k+1}} - \hat{v}_{i_k}}{\hat{x}_{i_{k+1}} - \hat{x}_{i_k}} \leq \frac{\hat{v}_{i_k} - \hat{v}_{i_{k-1}}}{x_{i_k} - \hat{x}_{i_{k-1}}}$ and let $\tilde{x}$ be the smallest value in T_p such that $\tilde{x} > \hat{x}_{i_k}$. Note that by Claim 2 in the Appendix, we will have $\hat{x}_{i_k} \notin T_P$. There will be two sub-cases. First, that $\hat{x}_{i_{k+1}} \leq \tilde{x}$ and second, that $\hat{x}_{i_{k+1}} > \tilde{x}$.

[Part 1, Case I.A: Right turn and candidate weakly less than next turning point.]

Consider the sub-case where $\hat{x}_{i_{k+1}} \leq \tilde{x}$. We will show that $V(\hat{x}_{i_{k+1}}) = U(\hat{x}_{i_{k+1}}, \hat{z}_{i_{k+1}})$. Assume by contradiction $V(\hat{x}_{i_{k+1}}) \neq U(\hat{x}_{i_{k+1}}, \hat{z}_{i_{k+1}})$ and let $m \in \mathbb{D}$ be such that $V(\hat{x}_{i_{k+1}}) = G^m(\hat{x}_{i_{k+1}}, \sigma^m(\hat{x}_{i_{k+1}}))$. Since $\tilde{x} \geq \hat{x}_{i_{k+1}}$, we have:

$$V(\hat{x}_{i_k}) = G^m(\hat{x}_{i_k}, \hat{z}_{i_k}),$$

$$\hat{x}'_{i_{k+1}} = f(\hat{x}_{i_{k+1}}, \sigma^q(\hat{x}_{i_{k+1}})),$$

for some q such that $m \neq q$. Now, by Assumption 1, Assumption 2 and using the reverse triangle inequality, we have

$$\begin{aligned} |\hat{x}'_{i_{k+1}} - \hat{x}'_{i_k}| &\geq \left| |\hat{x}'_{i_{k+1}} - f(\sigma^m(\hat{x}_{i_{k+1}}), \hat{x}_{i_{k+1}})| - |\hat{x}'_{i_k} - f(\sigma^m(\hat{x}_{i_{k+1}}), \hat{x}_{i_{k+1}})| \right| \\ &\geq |D - M(\hat{x}_{i_{k+1}} - \hat{x}_{i_k})|. \end{aligned}$$

Dividing through, and noting Assumption 3, we get

$$\frac{|\hat{x}'_{i_{k+1}} - \hat{x}'_{i_k}|}{\hat{x}_{i_{k+1}} - \hat{x}_{i_k}} \geq |\frac{D}{\hat{x}_{i_{k+1}} - \hat{x}_{i_k}} - M| > \frac{D}{\delta} - M.$$

However, this yields a contradiction to $\hat{x}_{i_{k+1}} \in \mathbb{X}$ by line 14 of Algorithm 1, implying $U(\hat{x}_{i_{k+1}}, \hat{z}_{i_{k+1}}) = V(\hat{x}_{i_{k+1}})$.

[Part 1, Case I.B: Right turn and candidate strictly greater than next turning point.]

Now consider the sub-case where $\hat{x}_{i_{k+1}} > \tilde{x}$. If $\hat{x}_{i_{k+1}}$ is the first point in $\hat{\mathbb{X}}$ such that $\hat{x}_{i_{k+1}} > \tilde{x}$, then $\hat{x}_{i_{k+1}}$ will be optimal and $\hat{x}_{i_{k+1}} \in \mathbb{X}^\star$ by Assumption 6 - item 1. On the other hand, suppose there exists x_s such that $\hat{x}_{i_{k+1}} > x_s > \tilde{x}$ and x_s is the smallest point in $\hat{\mathbb{X}}$ strictly greater than $\tilde{x}$. By Assumption 6 - item 1., $\hat{x}_s > \tilde{x}$ is optimal. Moreover, by Assumption 6 - item 2., we have

$$\frac{\hat{v}_s - \hat{v}_{i_k}}{\hat{x}_s - \hat{x}_{i_k}} \geq \frac{Q^q(x_s) - Q^m(\hat{x}_{i_k})}{\delta} = \frac{\hat{v}_s - \hat{v}_{i_k}}{\delta} > \frac{\hat{v}_{x_{i_k}} - \hat{v}_{x_{i_{k-1}}}}{\hat{x}_{i_k} - \hat{x}_{i_{k-1}}}, \tag{44}$$

where the first equality follows from Assumption 3. However, the above inequality implies that $x_s \in \mathbb{X}$, which is a contradiction to the assumption of this case that $\hat{x}_{i_{k+1}} > \tilde{x}$.

[Part 1, Case II: Left turn]

Let $\frac{\hat{v}_{i_{k+1}} - \hat{v}_{i_k}}{\hat{x}_{i_{k+1}} - \hat{x}_{i_k}} > \frac{\hat{v}_{i_k} - \hat{v}_{i_{k-1}}}{\hat{x}_{i_k} - \hat{x}_{i_{k-1}}}$. Then by Claim 1 in the Appendix, we must have that $U(\hat{x}_{i_{k+1}}, \hat{z}_{i_{k+1}}) = V(\hat{x}_{i_{k+1}})$, which implies $\hat{x}_{i_{k+1}} \in \mathbb{X}^\star$.

Part 2: Proof that $\hat{x}_i \in \mathbb{X} \Longleftarrow \hat{x}_i \in \mathbb{X}^\star$ holds for i with $i \leq l+1$.

Now we show that if a candidate point $\hat{x}_{l+1}$, with $\hat{x}_{l+1} \in \mathbb{X}^\star$ and $V(\hat{x}_{l+1}) = Q(\hat{x}_{l+1}, \hat{z}_{l+1})$, then $\hat{x}_{l+1} \in \mathbb{X}$. Consider the first case of a right turn.

[Part 2, Case I: Right turn]

Let $\frac{\hat{v}_{l+1} - \hat{v}_{i_k}}{\hat{x}_{l+1} - \hat{x}_{i_k}} \leq \frac{\hat{v}_{i_k} - \hat{v}_{i_{k-1}}}{\hat{x}_{i_k} - \hat{x}_{i_{k-1}}}$. By Claim 3 in the Appendix, we must have that $\hat{x}_{i_k} \notin T_P$. Suppose we have

$$V(\hat{x}_{i_k}) = G^m(\hat{x}_{i_k}, \hat{z}_{i_k}),$$

$$\hat{x}'_{l+1} = f(\hat{x}_{l+1}, \sigma_q(\hat{x}_{l+1})),$$

$$V(\hat{x}_{l+1}) = G^q(\hat{x}_{l+1}, \sigma_m(\hat{x}_{l+1})),$$

and $m = q$. By Assumption 2 and Assumption 3, we have

$$\frac{|\hat{x}'_{l+1} - \hat{x}'_{i_k}|}{|\hat{x}_{l+1} - \hat{x}_{i_k}|} \leq M < \frac{D}{\delta} - M.$$

Thus, by Algorithm 1, Line 14, we must have $\hat{x}_{l+1} \in \mathbb{X}$.

Alternatively, suppose $m \neq q$, then there exists $\tilde{x}$ such that $\hat{x}_{l+1} > \tilde{x} > \hat{x}_{i_k}$. By Assumption 6 - item 2., (44) will hold. However, this contradicts the assumption of this case that $\frac{\hat{v}_{l+1} - \hat{v}_{i_k}}{\hat{x}_{l+1} - \hat{x}_{i_k}} \leq \frac{\hat{v}_{i_k} - \hat{v}_{i_{k-1}}}{\hat{x}_{i_k} - \hat{x}_{i_{k-1}}}$.

[Part 2, Case II: Left turn]

Let $\frac{\hat{v}_{l+1} - \hat{v}_{i_k}}{\hat{x}_{l+1} - \hat{x}_{i_k}} > \frac{\hat{v}_{i_k} - \hat{v}_{i_{k-1}}}{\hat{x}_{i_k} - \hat{x}_{i_{k-1}}}$. By line 16 of Algorithm 1, we immediately have $\hat{x}_{l+1} \in \mathbb{X}$.

To conclude the proof, we have shown that if the claim given by (43) holds for all i with $i \leq l$, then it will hold for all i with $i \leq l+1$. Finally, note that by the assumption stated by the Proposition 1, $V(\hat{x}_i) = Q(\hat{x}_i, \hat{z}_i)$ for $i = 1, 2$ and $\hat{x}_i \in \mathbb{X}$ for $i \in \{0, 1\}$, thus the claim is true for $l = 2$. By the principle of induction, the claim given by (43) holds for all l, completing the proof ■

3.2.3 Discussion of assumptions

Assumption 1 is satisfied when the agent's policy function contains finitely many jumps. Assumption 2 is straightforward to satisfy in typical economic applications, where the policy function, conditional on a future stochastic sequence of discrete choices (σ^d), has a Lipshitz bound. This bound is commonly met since σ^d is the solution to a concave optimization problem, in which the optimal policy function exhibits well-defined maximal

and minimal marginal propensities to save (Carroll, 2023). Assumptions 3 and 4 are also satisfied for sufficiently large exogenous grid sizes if the distance between endogenous grid points decreases with a more refined exogenous grid (Dobrescu and Shanker, 2024).

Moreover, the forward and backward scans (illustrated in Figure 3 and discussed subsequently) implemented by FUES, along with the inclusion of approximate crossing points, serve as effective approximations of Assumptions 5 through 6, as demonstrated in Section 2.1. Specifically, the forward scan addresses violations of Assumption 6 - item 2, while the backward scan mitigates issues related to Assumption 6 - item 1. Furthermore, Assumption 6 - item 2 is generally satisfied with a sufficiently fine grid.[5]

4 Conclusions

This paper develops a fast upper envelope scan (FUES) method to solve any discrete-continuous stochastic dynamic optimization models where the optimization problem has a one-dimensional representation. FUES works by efficiently computing the upper envelope of the value correspondence generated by the EGM, overcoming the limitations of current methods that fail in applications involving non-monotonic policy functions. We demonstrate the wide applicability and massive computational advantages of FUES over competing upper envelope methods like DC-EGM (Iskhakov et al., 2017) and RFC (Dobrescu and Shanker, 2024), as well as over hybrid methods that use numerical optimization like NEGM (Druedahl, 2021) via three workhorse applications in the literature. Specifically, we find FUES to achieve computational speed gains of generally an order of magnitude above current methods, while maintaining solution accuracy. Moreover, in applications where DC-EGM cannot be applied due to non-monotonicity of the policy function, FUES also leads to up to an order of magnitude better Euler error over NEGM. Crucially, FUES scales well with model complexity, providing consistently high performance even when the endogenous grids become more irregular due to uncertainty or non-monotonicity.

One final remark relates to FUES being ultimately designed for models where the EGM grids of the potential solution points can be collapsed to one-dimensional ones, as it relies on the sequential ordering of points in the endogenous grid to perform the scan. This approach is not yet feasible in higher dimensions, where endogenous grids are irregular and lack a natural order for scanning. A promising area for future research is thus extending

[5]For $x^\star k + 1$ and $x^\star k$ close enough, $\frac{Q^m(x^\star k+1)-Q^q(x^\star k)}{x^\star k+1-x^\star k} < 0$. Taking the limit $\delta \to 0$ ensures this inequality holds, as $Q^{m,\prime}(x^\star k) < Q^{q,\prime}(x^\star k)$, satisfying the inequality in (42).

FUES to multiple dimensions by incorporating techniques such as Hilbert curves or other space-filling methods to produce an ordering of irregular multidimensional points.

References

Arellano, C. (2008). Default risk and income fluctuations in emerging economies. *American Economic Review*, 98(3):690–712.

Arellano, C., Maliar, L., Maliar, S., and Tsyrennikov, V. (2016). Envelope condition method with an application to default risk models. *Journal of Economic Dynamics and Control*, 69:436–459.

Attanasio, O., Levell, P., Low, H., and Sanchez-Marcos, V. (2018). Aggregating elasticities: Intensive and extensive margins of women's labor supply. *Econometrica*, 86(6):2049–2082.

Bacher, A., Grubener, P., and Nord, L. (2024). Joint search over the life cycle. *HOFIMAR Working Paper No. 5*.

Beraja, M. and Zorzi, N. (2024). Durables and size-dependence in the marginal propensity to spend. *NBER Working Paper No. 32080*.

Berger, D. and Vavra, J. (2015). Consumption dynamics during recessions. *Econometrica*, 83(1):101–154.

Brumm, J., Kotlikoff, L. J., and Krause, C. (2024). The global life-cycle optimizer: Analyzing fiscal policy's potential to rramatically ristort labor supply and saving. *NBER Working Paper No. 32335*.

Carroll, C. D. (2004). Theoretical Foundations of Buffer Stock Saving . *NBER Working Paper No. 10867*.

Carroll, C. D. (2006). The method of endogenous gridpoints for solving dynamic stochastic optimization problems. *Economics Letters*, 91(3):312–320.

Carroll, C. D. (2023). Theoretical foundations of buffer stock saving. *NBER Working Paper No. 10867*.

Carroll, C. D., Kaufman, A. M., Kazil, J. L., Palmer, N. M., and White, M. N. (2018). The Econ-ARK and HARK: Open Source Tools for Computational Economics. In Fatih Akici, David Lippa, Dillon Niederhut, and Pacer, M., editors, *Proceedings of the 17th Python in Science Conference*.

Coleman, W. J. (1990). Solving the stochastic growth model by policy-function iteration. *Journal of Business and Economic Statistics*, 8(1):27–29.

Cruces, L. (2024). A quantitative theory of the new life cycle of women's employment. *Journal of Economic Dynamics and Control*, page 104960.

Dobrescu, I. and Shanker, A. (2024). Discrete continuous high dimensional dynamic programming. *SSRN Working Paper No. 4850746*.

Dobrescu, L. I., Fan, X., Bateman, H., Newell, B. R., and Ortmann, A. (2016). Retirement savings: A tale of decisions and defaults. *Economic Journal*, 128(2016):1047–1094.

Dobrescu, L. I., Shanker, A., Bateman, H., Newell, B. R., and Thorp, S. (2024). Housing and pensions: Complements or substitutes in the portfolio allocation? *SSRN Working Paper No. 4069226*.

Druedahl, J. (2021). A guide on solving non-convex consumption-saving models. *Computational Economics*, 58:747–775.

Druedahl, J. and Jørgensen, T. H. (2017). A general endogenous grid method for multi-dimensional models with non-convexities and constraints. *Journal of Economic Dynamics and Control*, 74:87–107.

Fagereng, A., Holm, M. B., Natvik, G., and Moll, B. (2019). Saving behavior across the wealth distribution : The importance of capital gains. *NBER Working Paper No. 26588*.

Fella, G. (2014). A generalized endogenous grid method for non-smooth and non-concave problems. *Review of Economic Dynamics*, 17:329–344.

Iskhakov, F. (2015). Multidimensional endogenous gridpoint method: Solving triangular dynamic stochastic optimization problems without root-finding operations. *Economics Letters*, 135:72–76.

Iskhakov, F., Jørgensen, T. H., Rust, J., and Schjerning, B. (2017). The endogenous grid method for discrete-continuous dynamic choice models with (or without) taste shocks. *Quantitative Economics*, 8(2):317–365.

Iskhakov, F. and Keane, M. (2021). Effects of taxes and safety net pensions on life-cycle labor supply, savings and human capital: The case of Australia. *Journal of Econometrics*, 223(2):401–432.

Jang, Y. and Lee, S. (2023). A generalized endogenous grid method for default risk models. *SSRN Working Paper No. 3442070*.

Judd, K. L. (1992). Projection methods for solving aggregate growth models. *Journal of Economic Theory*, 58(2):410–452.

Kaplan, G., Mitman, K., and Violante, G. L. (2020). The housing boom and bust: Model meets evidence. *Journal of Political Economy*, 128(9):3285–3345.

Kaplan, G. and Violante, G. L. (2014). A model of the consumption response to fiscal stimulus payments. *Econometrica*, 82(4):1199–1239.

Khan, A. and Thomas, J. K. (2008). Idiosyncratic shocks and the role of nonconvexities in plant and aggregate investment dynamics. *Econometrica*, 76(2):395–436.

Kovacs, A., Low, H., and Moran, P. (2021). Estimating temptation and commitment over the life cycle. *International Economic Review*, 62(1):101–139.

Laibson, D., Maxted, P., and Moll, B. (2021). Present bias amplifies the household balance-sheet channels of macroeconomic policy. *NBER Working Paper No. 29094*.

Le Blanc, J., Slacalek, J., and White, M. N. (2023). Housing wealth across countries: The role of expectations, preferences and institutions. *mimeo*.

Li, H. and Stachurski, J. (2014). Solving the income fluctuation problem with unbounded rewards. *Journal of Economic Dynamics and Control*, 45:353–365.

Skiba, A. K. (1978). Optimal growth with a convex-concave production function. *Econometrica*, 46(3):527–539.

White, M. N. (2015). The method of endogenous gridpoints in theory and practice. *Journal of Economic Dynamics and Control*, 60:26–41.

Yogo, M. (2016). Portfolio choice in retirement: Health risk and the demand for annuities, housing, and risky assets. *Journal of Monetary Economics*, 80:17–34.

Online Appendix

A Endogenous grid-specific jump detection

In practice, we find that selecting a reasonable constant value for $\bar{M}$ through experimentation (and subsequently verifying the upper envelope is recovered) works well. However, an endogenous jump detection threshold $\bar{M}_i^\star$ can also be theoretically derived based on the curvature of the policy functions, and easily computed for each grid point. To this effect, note that the role of the jump detection threshold is to detect a point $\hat{x}_{i+1}$ that does not lie on the same future choice-specific policy function as $\hat{x}_i$. Consider now that for any real-valued continuously differentiable function f on an interval I, by the Mean Value Theorem, we must have that $|f(y) - f(x)| \leq L|y - x|$, where $L = \sup\{|f'(z)| : z \in I\}$. Let $\sigma_t^{\mathbf{d}}$ be the asset policy function at time t, conditional on a future sequence of discrete choices $\mathbf{d}$ (recall the discussion below (5)). The functions $a \mapsto \sigma_t^{\mathbf{d}}(a)$ are continuously differentiable and convex (Carroll, 2004) since all future discrete choices are held fixed. For any exogenous grid point $\hat{x}_{i+1}$ to imply the same future discrete choices as $\hat{x}_i$, we must then have that

$$|\sigma_t^{\mathbf{d}_i}(\hat{x}_i) - \sigma_t^{\mathbf{d}_{i+1}}(\hat{x}_{i+1})| \leq \bar{M}_i^\star |\hat{x}_{i+1} - \hat{x}_i|, \tag{45}$$

where $\bar{M}_i^\star = \max\left\{\left|\partial\sigma^{\mathbf{d}_{i+1}}(\hat{x}_{i+1})\right|, \left|\partial\sigma^{\mathbf{d}_i}(\hat{x}_i)\right|\right\}$ and we use ∂ to denote the derivative of the policy function with respect to financial assets. The term $\mathbf{d}_i$ above is the future sequence of discrete choices implied by the exogenous grid point i. If two points do not satisfy the above inequality, then they cannot lie on the same future choice-specific policy function and we have 'detected a jump' in the policy function.

Starting from the exogenous grid points, we can use the Euler equation for the problem to derive the terms $\partial\sigma^{\mathbf{d}_i}(\hat{x}_i)$ analytically and recursively as follows:

$$\partial\sigma_t^{\mathbf{d}_i}(\hat{x}_i) = \frac{(1+r)u''(\hat{c}_i)}{u''(\hat{c}_i) + \beta(1+r)u''(\hat{c}_i')[(1+r) - \partial\sigma_{t+1}^{\mathbf{d}_i}(\hat{x}_i')]}, \tag{46}$$

where $\hat{c}_i'$ is the next period consumption implied by the exogenous grid point i. It is important to note that the dependence of the policy function derivatives $\partial\sigma_t^{\mathbf{d}_i}$ on the future sequence of discrete choices is *given implicitly* by the exogenous grid point i. Thus, the above derivative can be calculated by evaluating the RHS of the equation above as follows: (i) evaluate $u''(\hat{c}_i)$ using the $\hat{c}_i$ implied by the standard EGM step, and then (ii)

evaluate the next period value $u''(\hat{c}'_i)\left[(1+r)-\partial\sigma^{\mathbf{d}_i}_{t+1}(\hat{x}'_i)\right]$ using an interpolant of the function $u''(c')[(1+r)-\partial\sigma^{\mathbf{d}}_{t+1}(x')]$. In what follows, at a time t iteration, the function $u''(c')\left[(1+r)-\partial\sigma^{\mathbf{d}}_{t+1}(x')\right]$ is evaluated on the exogenous grid points and stored in a grid $\hat{\mathbb{O}}'_t$. (For period T, we can use $\partial\sigma^{\mathbf{d}}_T = 0$ since all wealth is consumed.) In particular, fixing a time t and noting $\hat{o}'_i \in \hat{\mathbb{O}}'_t$, define:

$$\hat{\Delta}_i = \frac{(1+r)u''(\hat{c}_i)}{u''(\hat{c}_i)+\beta(1+r)\hat{o}'_i} \approx \partial\sigma^{\mathbf{d}_i}_t(\hat{x}_i), \tag{47}$$

$$\hat{o}_i = u''(\hat{c}_i)\left[(1+r)-\hat{\Delta}_i\right]. \tag{48}$$

Using the above, $\hat{\mathbb{O}}_t$ can be constructed from the points $\hat{o}_i$. The modified pseudo-code for FUES with endogenous jump detection becomes:[6]

Box 2: FUES method with endogenous jump detection

1. Compute $\hat{\mathbb{X}}_t$, $\hat{\mathbb{C}}_t$, $\hat{\mathbb{V}}_t$, $\hat{\mathbb{O}}_t$, $\hat{\mathbb{X}}'_t$, $\hat{\mathbb{C}}'$ and $\hat{\mathbb{O}}'_t$ using standard EGM.
2. Sort all sequences in order of the *endogenous* grid $\hat{\mathbb{X}}_t$.
3. Start from point $i = 2$.
4. Compute $g_i = \frac{\hat{v}_i - \hat{v}_{i-1}}{\hat{x}_i - \hat{x}_{i-1}}$, $g_{i+1} = \frac{\hat{v}_{i+1} - \hat{v}_i}{\hat{x}_{i+1} - \hat{x}_i}$, $\hat{\Delta}_i$, and $\hat{\Delta}_{i+1}$.
5. If the endogenous bound in (45) is violated and a right turn is made ($g_{i+1} < g_i$), then remove point $i+1$ from grids $\hat{\mathbb{X}}_t$, $\hat{\mathbb{V}}_t$, $\hat{\mathbb{O}}_t$, $\hat{\mathbb{X}}'_t$ and $\hat{\mathbb{O}}'_t$. Otherwise, set $i = i+1$.
6. If $i+1 \leq |\hat{\mathbb{X}}_t|$, then repeat from step 5.

Once the scan is complete for time t, the refined grid $\mathbb{O}_t$ can be interpolated on the refined endogenous grid along with the refined value and policy function. We also note that if the policy functions are Lipshitz and there are only finitely many jumps, then the grid-specific bounds will be bounded and we will have effectively chosen a bound at each grid point such that the jump detection threshold at Assumption 4 in Section 3 is satisfied. Hence, for a grid size large enough, FUES will eliminate all sub-optimal points without error.

B Intermediate proofs

The first intermediate result says that if a point makes a left turn from an optimal point, then it is also optimal.

[6]The FUES implementation with endogenous jump detection is provided as an additional option here.

Claim 1 *Fix the triple $\hat{x}_i, \hat{x}_{i+1}, \hat{x}_{i+2}$ for some i and assume $\hat{x}_i, \hat{x}_{i+1} \in \mathbb{X}^\star$. If we have that*

$$\frac{\hat{v}_{i+1} - \hat{v}_i}{\hat{x}_{i+1} - \hat{x}_i} < \frac{\hat{v}_{i+2} - \hat{v}_{i+1}}{\hat{x}_{i+2} - \hat{x}_{i+1}}, \tag{49}$$

then $\hat{x}_{i+2} \in \mathbb{X}^\star$.

Proof. Fix l, with $l \in \mathbb{D}$ and such that $V(\hat{x}_{i+1}) = G^l(\hat{x}_{i+1}, \sigma^l(\hat{x}_{i+1}))$. Suppose by contradiction that $\hat{x}_{i+2} \notin \mathbb{X}^\star$. Suppose first that $V(\hat{x}_i) = G^l(\hat{x}_i, \sigma^l(\hat{x}_i))$. Since $\hat{x}_{i+2} \notin \mathbb{X}^\star$, we must have $\hat{v}_{i+2} = G^m(\hat{x}_{i+2}, \sigma^m(\hat{x}_{i+2}))$ and $m \neq l$. By concavity and (49), we must have $G^m(\hat{x}_{i+2}, \sigma^m(\hat{x}_{i+2})) > G^l(\hat{x}_{i+2}, \sigma^l(\hat{x}_{i+2}))$. This implies that $V(\hat{x}_{i+2}) = G^p(\hat{x}_{i+2}, \sigma^p(\hat{x}_{i+2}))$ for $p \neq l$ and $p \neq m$. Moreover, the functions G^p and G^l must cross at some point $\tilde{x}_i \in T_p$, with $\tilde{x}_i \in [\hat{x}_{i+1}, \hat{x}_{i+2})$. However, we have now violated Assumption 6 - item 1., since $\hat{x}_{i+2}$ is the first point after a crossing point and must be optimal.

Now suppose $V(\hat{x}_i) = G^b(\hat{x}_i, \sigma^b(\hat{x}_i))$ for some $b \neq l$. This implies a crossing point $\tilde{x}$ satisfies $\tilde{x} \in (\hat{x}_i, \hat{x}_{i+1})$. However, $\tilde{x} \in (\hat{x}_i, \hat{x}_{i+1})$ also yields a contradiction since by Assumption 5, we must have $\tilde{x} \in \mathbb{X}^\star$. ■

Claim 2 *Consider the setting of Part 1 of the proof of Proposition 1. Let $\tilde{x}$ be the smallest value in T_p such that $\tilde{x} > \hat{x}_{i_k}$. If $\frac{\hat{v}_{i_{k+1}} - \hat{v}_{i_k}}{\hat{x}_{i_{k+1}} - \hat{x}_{i_k}} \leq \frac{\hat{v}_{i_k} - \hat{v}_{i_{k-1}}}{x_{i_k} - \hat{x}_{i_{k-1}}}$, then $\hat{x}_{i_k} \notin T_P$.*

Proof. Suppose by contradiction that $\hat{x}_{i_k} \in T_P$. By Assumption 6 - item 2, we must have that $\hat{x}_{i_k+1} \in \mathbb{X}^\star$ and that

$$\frac{\hat{v}_{i_k+1} - \hat{v}_{i_k}}{\hat{x}_{i_k+1} - \hat{x}_{i_k}} \geq \frac{Q^q(x_{i_k+1}) - Q^m(x_{i_k})}{\delta} = \frac{\hat{v}_{i_k+1} - \hat{v}_{i_k}}{\delta} > \frac{\hat{v}_{x_{i_k}} - \hat{v}_{x_{i_{k-1}}}}{x_{i_k} - x_{i_{k-1}}}, \tag{50}$$

where q and m are elements of $\mathbb{D}$ that satisfy the notation from Definition 1 with $\hat{x}_{i_k}$ as the turning point. To complete the proof, since the above equation implies $i_k + 1$ makes a left turn from the point i_k and i_{k-1} on the value correspondence, by Line 9 of Algorithm 1, we have that $\hat{x}_{i_k+1} \in \mathbb{X}$, $\hat{x}_{i_k+1} \in \mathbb{X}^\star$ and $i_{k+1} = i_k$. However, this contradicts the assumption of the claim that x_{i_k} makes a right turn on the value correspondence. Thus, $\hat{x}_{i_k} \notin T_P$. ■

The proof for the following claim is analogous to Claim 2, replacing $i_k + 1$ with $l + 1$.

Claim 3 *Consider the setting of Part 1 of the proof of Proposition 1. Let $\hat{x}_{l+1}$, with $\hat{x}_{l+1} \in \mathbb{X}^\star$ and $V(\hat{x}_{l+1}) = G(\hat{x}_{l+1}, \hat{z}_{l+1})$. If $\tilde{x}$ is the smallest value in T_p such that $\tilde{x} > \hat{x}_{i_k}$, then $\hat{x}_{i_k} \notin T_P$. If $\frac{\hat{v}_{l+1} - \hat{v}_{i_k}}{x_{l+1} - \hat{x}_{i_k}} \leq \frac{\hat{v}_{i_k} - \hat{v}_{i_{k-1}}}{x_{i_k} - \hat{x}_{i_{k-1}}}$, then $\hat{x}_{i_{l+1}} \notin T_P$.*

C Additional tables and figures

Table 5: Speed and accuracy of FUES in the continuous housing investment with adjustment frictions model with infinite horizon.

Grid Size A	τ	*Time per iteration*			*Euler error*		
		RFC	**FUES**	**NEGM**	**RFC**	**FUES**	**NEGM**
300	0.03	7.713	6.871	11.336	-3.799	-3.506	-2.338
	0.07	7.639	6.734	10.932	-3.037	-2.945	-2.061
	0.15	7.846	6.829	10.833	-2.357	-2.303	-1.680
400	0.03	10.537	9.269	15.285	-3.756	-3.533	-2.386
	0.07	10.429	9.370	14.707	-3.035	-2.938	-2.102
	0.15	10.504	9.468	14.804	-2.358	-2.305	-1.699
500	0.03	12.290	10.609	17.247	-3.727	-3.408	-2.402
	0.07	11.998	10.558	16.975	-3.028	-2.862	-2.106
	0.15	12.044	10.589	20.991	-2.356	-2.298	-1.704

Table 6: Model parameters: $\gamma = 3$, $\alpha = 0.66$, $\beta = 0.93$, $\tau = 0.18$, $r = 0.01$, $\bar{\theta} = 1.34$. FUES jump detection threshold is $\bar{M} = 1.2$, with a 4-step forward and backward scan used. RFC jump detection threshold is $\bar{M} = 1.2$, with a search radius of 0.75. Time per iteration is reported in seconds, while mean Euler error is reported in decimal logarithms (Judd, 1992; Fella, 2014; Druedahl and Jørgensen, 2017).

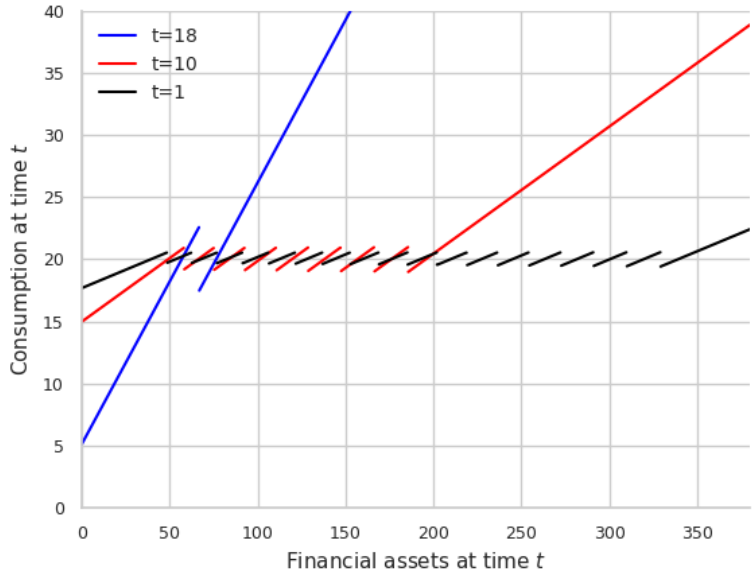

Figure 8: Optimal consumption functions without smoothing for workers in Application 1.

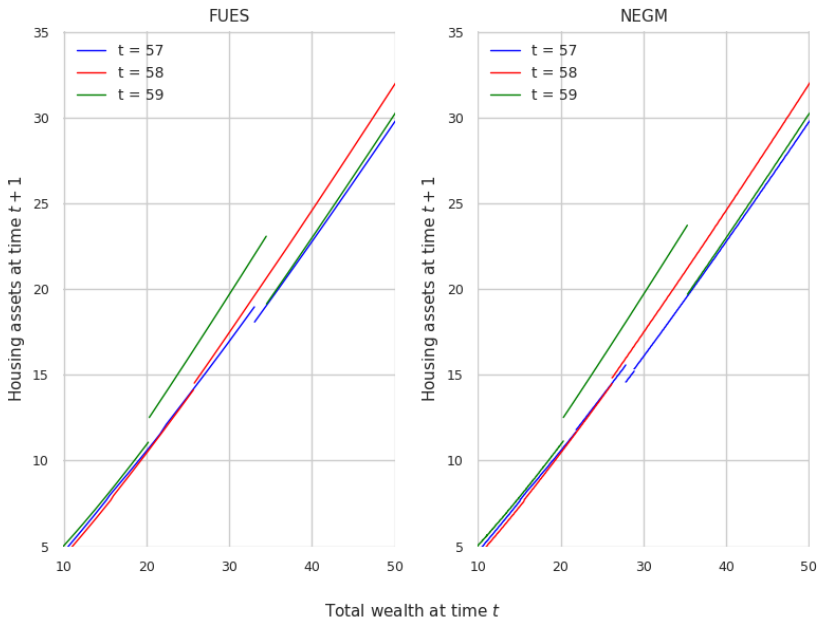

Figure 9: Housing policy functions in Application 2 computed using FUES and NEGM. Financial assets and housing grid sizes are both 600.

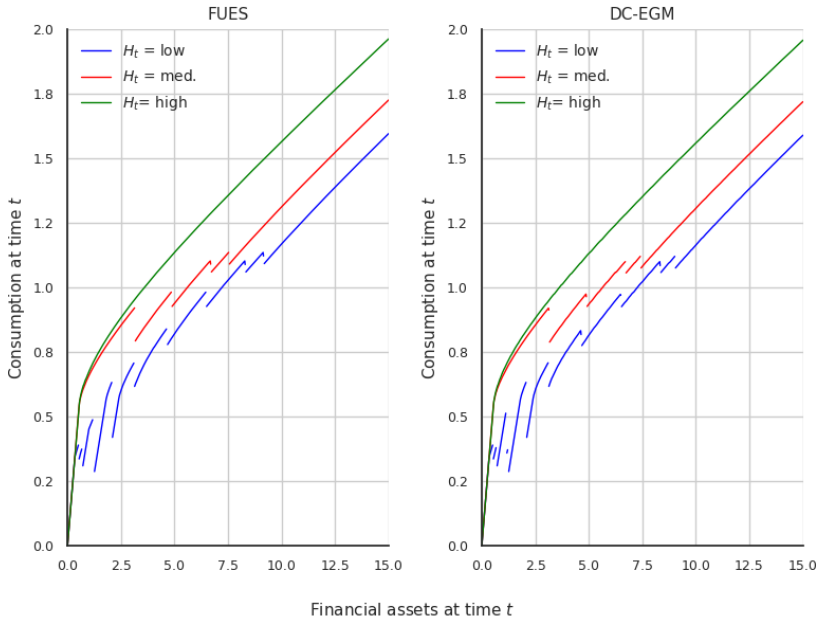

Figure 10: Consumption policy function in Application 3 computed using FUES and DC-EGM. The plot uses the lowest wage shock and three housing levels at the start of period t. Financial assets grid size is 2,000, while housing grid size is 10.